H2GEO

H2GEO

New technology for hydrogen and geopolymer composites production from post-mining waste

Deliverable 3.2

Physicochemical analyses and mechanical property tests of the separation products

Grant agreement No: 101112386

03.2024

Authors:

Joanna CAŁUS MOSZKO Ph.D.	Główny Instytut Górnictwa – Państwowy Instytut Badawczy *Central Mining Institute National Research Institute*
Agnieszka KLUPA Ph.D.	Główny Instytut Górnictwa – Państwowy Instytut Badawczy *Central Mining Institute National Research Institute*
Magdalena CEMPA Ph.D.	Główny Instytut Górnictwa – Państwowy Instytut Badawczy *Central Mining Institute National Research Institute*
Krzysztof WIERZCHOWSKI Ph.D.	Główny Instytut Górnictwa – Państwowy Instytut Badawczy *Central Mining Institute National Research Institute*
Henryk ŚWINDER Ph.D.	Główny Instytut Górnictwa – Państwowy Instytut Badawczy *Central Mining Institute National Research Institute*
Piotr MATUSIAK Ph.D.	INSTYTUT TECHNIKI GÓRNICZEJ KOMAG *KOMAG Institute of Mining Technology*
Daniel KOWOL Ph.D.	INSTYTUT TECHNIKI GÓRNICZEJ KOMAG *KOMAG Institute of Mining Technology*
Rafał BARON	INSTYTUT TECHNIKI GÓRNICZEJ KOMAG *KOMAG Institute of Mining Technology*
Paweł FRIEBE	INSTYTUT TECHNIKI GÓRNICZEJ KOMAG *KOMAG Institute of Mining Technology*
Olga ZIÓŁKOWSKA	INSTYTUT TECHNIKI GÓRNICZEJ KOMAG *KOMAG Institute of Mining Technology*
Martin PALOU	Slovenská akadémia vied - Institute of Construction and Architecture
Joanna BIGDA	Institute of Energy and Fuel Processing Technology (ITPE)
Karina IGNASIAK	Institute of Energy and Fuel Processing Technology (ITPE)
Janusz LASEK	Institute of Energy and Fuel Processing Technology (ITPE)
Krzysztof SUPERNOK	Institute of Energy and Fuel Processing Technology (ITPE)
Małgorzata WOJTASZEK-KALAITZIDI	Institute of Energy and Fuel Processing Technology (ITPE)
Katarzyna RYCHLEWSKA	Institute of Energy and Fuel Processing Technology (ITPE)
Agata CZARDYBON	Institute of Energy and Fuel Processing Technology (ITPE)
Krzysztof GŁÓD	Institute of Energy and Fuel Processing Technology (ITPE)

Table of Contents

List of Tables:

List of Figures:

Introduction

As part of Task T3.2, research was conducted following the methodology outlined in D2.2, ensuring consistency in procedures and objectives. The samples analysed consisted of the mineral fraction of waste from the tailings of three different locations: Paskov, Karvina, and Haldex. These waste materials underwent a gravity separation process at both laboratory and semi-industrial scales using a mineral concentrator. The research was conducted by KOMAG, the project leader, known for its expertise in coal beneficiation and raw material recovery from waste.

Gravity Separation Process and Sample Preparation

The gravity separation process allowed for the segregation of two main material fractions: the mineral fraction and the coal fraction. This method, widely used in the coal and mineral industries, facilitated coal beneficiation and the recovery of valuable raw materials from mine tailings. The separation resulted in materials with varying densities and chemical compositions, enabling further detailed evaluation of their properties.

The objective of this research was to assess the chemical composition and physicochemical properties (including mechanical properties) of the separated fractions. The analysis aimed to determine the potential for raw material recovery from mine tailings and evaluate their suitability for industrial applications such as construction material production, coal beneficiation, or other uses. The outcomes of these studies will contribute to assessing the separation process's efficiency and identifying optimal strategies for raw material recovery.

For this task, samples obtained during T3.1 were analyzed. These samples were products of the laboratory jigging enrichment process. Based on previous tests, three materials—Haldex 1, Haldex 2, and Karvina 2—were selected for research in T3.2. Each material, with a grain size of 30–3 mm, was separated in the laboratory jig into two products: a concentrate primarily composed of coal grains and a waste product primarily composed of mineral grains. The concentrate was referred to as the

combustible product, while the waste product was referred to as the mineral product. The methodology for conducting tests using the laboratory jig is described in Deliverable Report D3.1, *Results of Laboratory Tests of Mine Wastes of Jig Beneficiation*.

Each obtained product was homogenized, divided into four equal parts, and sent to project partners for planned laboratory studies (ITPE, GIG, USTARCH, KOMAG). All partners received concentrate samples weighing approximately 6 kg and waste product samples weighing approximately 20 kg each.

Laboratory Analyses Conducted

KOMAG Institute of Mining Technology

The following analyses were conducted:

Sieve analysis using sieves with hole sizes of 20, 10, and 6 mm, resulting in grain classes: 30–20 mm, 20–10 mm, 10–6 mm, and 6–3 mm.

Density analysis in heavy liquids (aqueous solution of zinc chloride) with densities of 1.5 and 1.8 g/cm³, yielding fractions: <1.5, 1.5–1.8, and >1.8 g/cm³.

Determination of physicochemical properties in density fraction, including:

- Water content
- Ash content
- Sulfur content
- Heat of combustion, including calculated calorific value

Similar determinations were also performed for the previously separated grain size classes (30–10 mm and 10–3 mm). Based on the obtained values, the average contents of the analyzed parameters were calculated for each grain size class and for the entire material, using a weighted arithmetic mean.

All analyses were conducted according to the following applicable standards:

- Grain analysis: **PN-ISO 1953:1999**
- Density analysis: **PN-G-04559:1997**

- Determination of water content: **PN-ISO 589:2006**
- Determination of ash content: **PN-ISO 1171:2002**
- Determination of total sulfur content: **PN-G-04584:2001**
- Determination of heat of combustion: **PN-ISO 1928:2020-05**

The laboratory tests complied with the requirements of **PN-EN ISO/IEC 17025:2018-02** and were conducted using calibrated measuring equipment as D.2.2.

GIG Central Mining Institute

The following analyses were conducted:

Sieve analysis using sieves with hole sizes of 32, 16, 8, and 4 mm, resulting in grain classes: >32 mm, 32–16 mm, 16–8 mm, 8–4 mm, and <4 mm.

- **Mechanical property tests**:
  - Crushing resistance of aggregates (Los Angeles Index)
  - Wear resistance of aggregates (micro-Deval)
  - Water absorption
  - Frost resistance
- **SEM/EDS analysis**

All analyses adhered to the following applicable standards:

- Los Angeles Index: **PN-EN 1097-2**
- Abrasion resistance: **PN-EN 1097-1**
- Water absorption: **PN-EN 1097-6**
- Frost resistance: **PN-EN 1367-1**
- SEM/EDS Analysis: Analysis according to the proprietary methodology. The laboratory tests were carried out in accordance with the requirements of the **PN-EN ISO/IEC 17025:2018-02** standard using measuring equipment ensuring consistency of measurements. The research used supervised measurement equipment, including SEM-SU3500 from Hitachi.

ITPE Institute of Energy and Fuel Processing Technology performed the following analyses:

- Proximate and ultimate analysis, chemical composition, and characteristic ash fusion temperatures
- Microscopic evaluation using a polarizing microscope
- Trace element content determination (Be, Co, Eu, Ga, Mg, Sb, Mo, Ni, Sc, Sm, W, Y, Yb, Sr, Li, Ti)
- Main element content: Si, Al, Na, K
- Heavy metal content in the coal fraction

These analyses were performed using the same equipment and methodology described in D2.2.

Sample Identification

Coal Fraction:

- Carbon-bearing jig product Haldex 1 – coal fraction from Haldex 1 waste heap
- Carbon-bearing jig product Haldex 2 – coal fraction from Haldex 2 waste heap
- Carbon-bearing jig product Karvina 2 – coal fraction from Karvina 2 waste heap
- HALDEX – Material for gasification (Task 4.2, additionally analyzed)

Mineral Fraction:

- Mineral jig product Haldex 1 – mineral fraction from Haldex 1 waste heap
- Mineral jig product Haldex 2 – mineral fraction from Haldex 2 waste heap
- Mineral jig product Karvina 2 – mineral fraction from Karvina 2 waste heap
- HALDEX – Material for calcination (Task 5.1, additionally analyzed)

The results of these analyses will contribute to evaluating the efficiency of the separation process and optimizing strategies for raw material recovery.

1. Test results

The results of sample analyses are presented in the following subsections, in a tabular form, with division for each sample into the results of granulometric-qualitative and density-qualitative analyses.

1.1. Haldex 1 product samples

The product samples were obtained from the jig separation of material collected from the Panewnicka heap, and the sampling location is shown in Figure 1.

Figure 1 Place of collecting the sample Haldex 1 - 50.216813N, 18.886416E.

1.1.1. Results of granulometric-qualitative analysis

In the grain size classes obtained from the granulometric analysis of the samples, the moisture content, ash content, sulphur content, calorific value, and heating value (in the analytical state) were determined. The analysis results for the carbon-bearing product are presented in Table 1, and for the mineral product in Table 2.

Table 1. Granulometric-qualitative composition of the carbon-bearing product.

Grain class	Share	Moisture content, W^a	Ash content, A^a	Sulphur content, S^a	Heat of combustion, Q_s^a	Calorific value, Q_i^a
mm	%	%	%	%	kJ/kg	kJ/kg
30-20	12.07	2.01	18.32	0.89	26845	25856
20-10	25.51	1.58	17.10	0.76	27335	26337
10-6	30.95	1.73	20.45	0.73	25925	24964
6-3	31.47	1.69	27.32	0.64	23258	22379
Sum	100.00					
Average		1.71	21.50	0.73	25556	24608

In the analysed material, the smallest share, equal to 12.07%, was constituted by grains in the 30-20 mm class. The shares of the remaining grain size classes ranged from 25.51% (20-10 mm) to 31.47% (6-3 mm). The average sulphur content in the analysed sample was 0.73%, with the highest content observed in the 30-20 mm class, at 0.89%. Ash content ranged from 17.10% (20-10 mm class) to 27.32% (6-3 mm class). The lowest ash content corresponded to the most favourable calorific value, equal to 26337 kJ/kg (20-10 mm class). The average ash content and calorific value were 21.50% and 24608 kJ/kg, respectively.

Table 2 Granulometric-qualitative composition of the mineral product.

Grain class	Share	Moisture content, W^a	Ash content, A^a	Sulphur content, S^a	Heat of combustion, Q_s^a	Calorific value, Q_i^a
mm	%	%	%	%	kJ/kg	kJ/kg
30-20	21.97	1.12	86.09	0.37	1258	1080
20-10	29.77	1.25	83.67	0.58	2158	1950
10-6	25.13	1.00	82.19	0.66	2803	2580
6-3	23.13	1.22	81.89	0.74	2825	2596
Sum	100.00					
Average		1.15	83.42	0.59	2277	2066

1.

The largest share of grains was represented by the 20-10 mm size class (29.77%), while the smallest share was in the 30-20 mm class (21.97%). The ash content in the waste was significantly higher than in the combustible product, ranging from 81.89% (for the 6-3 mm class) to 86.09% (for the 30-20 mm class). The average ash content for the entire waste sample was 83.42%, which is nearly four times higher than in the combustible product.

The average sulphur content in the waste was 0.59%, a lower value compared to the combustible product. The average calorific value of the waste was nearly 12 times lower than that of the combustible product, amounting to 2066 kJ/kg.

1.1.2. Results of density-qualitative analysis

Tables 3-5 (for the carbon-bearing product) and tables 6-8 (for the mineral product) present the results of density-qualitative analyses for selected grain size classes.

Combustible product

Table 3 Density-qualitative composition of the carbon-bearing product in grain class 30-10 mm.

Density fraction	Share	Moisture content, W^a	Ash content, A^a	Sulphur content, S^a	Heat of combustion, Q_s^a	Calorific value, Q_i^a
g/cm³	%	%	%	%	kJ/kg	kJ/kg
<1.5	68.89	1.84	8.05	0.86	30970	29862
1.5-1.8	25.12	1.68	34.84	0.81	20501	19710
>1.8	5.99	1.59	59.00	0.46	11958	11454
Sum	100.00					
Average		1.78	17.83	0.82	27201	26209

Table 4 Density-qualitative composition of the carbon-bearing product in grain class 10-3 mm.

Density fraction	**Share**	**Moisture content, W^a**	**Ash content, A^a**	**Sulphur content, S^a**	**Heat of combustion, Q_s^a**	**Calorific value, Q_i^a**
g/cm³	%	%	%	%	kJ/kg	kJ/kg
<1.5	62.97	1.85	9.52	0.80	30062	28971
1.5-1.8	16.88	1.83	35.44	0.74	19408	18623
>1.8	20.16	1.78	61.12	0.37	10829	10348
Sum	100.00					
Average		1.83	24.29	0.71	24388	23471

Table 5 Density-qualitative composition of the carbon-bearing product in grain class 30-3 mm.

Density fraction	**Share**	**Moisture content, W^a**	**Ash content, A^a**	**Sulphur content, S^a**	**Heat of combustion, Q_s^a**	**Calorific value, Q_i^a**
g/cm³	%	%	%	%	kJ/kg	kJ/kg
<1.5	65.19	1.84	8.97	0.83	30403	29306
1.5-1.8	19.97	1.78	35.21	0.76	19819	19032
>1.8	14.83	1.71	60.32	0.41	11253	10764
Sum	100.00					
Average		1.81	21.83	0.75	25449	24503

In the analysed material within the grain size class of 30-3 mm, a predominant share of combustible fractions with a density of <1.8 g/cm³ (>85%) was observed. The proportion of fractions >1.8 g/cm³ was noticeably higher in the 10-3 mm grain size class (20.16%). The average ash content in the analysed classes 30-10 mm, 10-3 mm, and, consequently, 30-3 mm was 17.83%, 24.29%, and 21.83%, respectively. The lowest sulphur content was found in fractions with a density >1.8 g/cm³, amounting to 0.46% and 0.37% for the 30-10 mm and 10-3 mm classes, respectively. The average sulphur content in the analysed grain size classes was 0.82%, 0.71%, and 0.75%.

Mineral product

Table 6 Density-qualitative composition of the mineral product in grain class 30-10 mm.

Density fraction	Share	Moisture content, W^a	Ash content, A^a	Sulphur content, S^a	Heat of combustion, Q_s^a	Calorific value, Q_i^a
g/cm³	%	%	%	%	kJ/kg	kJ/kg
<1.5	0.49	1.67	11.18	0.71	30003	28933
1.5-1.8	2.31	1.92	39.41	1.45	18427	17687
>1.8	97.19	1.04	86.58	0.47	1212	1040
Sum	100.00					
Average		1.06	85.12	0.49	1752	1563

Table 7 Density-qualitative composition of the mineral product in grain class 10-3 mm

Density fraction	Share	Moisture content, W^a	Ash content, A^a	Sulphur content, S^a	Heat of combustion, Q_s^a	Calorific value, Q_i^a
g/cm³	%	%	%	%	kJ/kg	kJ/kg
<1.5	1.42	1.69	10.09	0.78	29921	28838
1.5-1.8	2.94	1.55	37.78	0.78	18899	18145
>1.8	95.64	1.10	84.98	0.75	1584	1393
Sum	100.00					
Average		1.12	82.53	0.75	2495	2275

Table 8 Density-qualitative composition of the mineral product in grain class 30-3 mm.

Density fraction	Share	Moisture content, W^a	Ash content, A^a	Sulphur content, S^a	Heat of combustion, Q_s^a	Calorific value, Q_i^a
g/cm³	%	%	%	%	kJ/kg	kJ/kg
<1.5	0.94	1.68	10.65	0.75	29963	28887
1.5-1.8	2.62	1.74	38.62	1.13	18654	17908
>1.8	96.44	1.07	85.81	0.61	1392	1211
Sum	100.00					
Average		1.09	83.87	0.62	2112	1907

A small share of combustible fractions was observed in the analysed samples, with material predominantly consisting of density fractions >1.8 g/cm³ (averaging 96.44%). The ash content was directly proportional to the increasing density fraction, with an average of 83.87%. Comparing individual grain size classes, the 10-3 mm class showed slightly lower ash content, which is associated with a higher share of combustible fractions, amounting to 4.36%. The average sulphur content was somewhat lower compared to the combustible product, at 0.62%. The waste material was characterized by a significantly lower average calorific value (1907 kJ/kg for the 30-3 mm grain size class) compared to the combustible product, whose value was nearly 13 times higher.

1.2. Haldex 2 product samples

The product samples were obtained from the jig separation of material collected from the Panewnicka heap, and the sampling location is shown in Figure 2.

Figure 2 Place of collecting the sample Haldex 2 - 50.215263N, 18.886639E

1.2.1. Results of granulometric-qualitative analysis

In the grain size classes obtained from the granulometric analysis of the samples, the moisture content, ash content, sulphur content, calorific value, and heating value (in the analytical state) were determined. The analysis results for the carbon-bearing product are presented in Table 9, and for the mineral product in Table 10.

Table 9 Granulometric-qualitative composition of the carbon-bearing product sample.

Grain class	Share	Moisture content, W^a	Ash content, A^a	Sulphur content, S^a	Heat of combustion, Q_s^a	Calorific value, Q_i^a
mm	%	%	%	%	kJ/kg	kJ/kg
30-20	34.09	1.76	17.19	0.84	26185	25186
20-10	38.82	1.54	19.13	0.91	26686	25712
10-6	16.74	1.44	22.16	0.64	25647	24710
6-3	10.35	1.95	28.81	0.77	22098	21233
Sum	100.00					
Average		1.64	19.98	0.83	25866	24901

In the analysed material, the smallest shares were observed in the 6-3 mm and 10-6 mm size classes, accounting for 10.35% and 16.74%, respectively. The shares of the remaining size classes were 34.09% (30-20 mm) and 38.82% (20-10 mm). The ash content was inversely proportional to the grain size, ranging from 17.19% (for the 30-20 mm size class) to 28.81% (for the 6-3 mm size class). The average sulphur content was 0.83%. The calorific value was directly proportional to the grain size, with an average value of 24901 kJ/kg.

Table 10 Granulometric-qualitative composition of the mineral product

Grain class	Share	Moisture content, W^a	Ash content, A^a	Sulphur content, S^a	Heat of combustion, Q_s^a	Calorific value, Q_i^a
mm	%	%	%	%	kJ/kg	kJ/kg
30-20	29.99	0.99	82.58	0.62	2680	2462
20-10	35.73	0.92	84.19	0.81	2311	2113
10-6	17.94	1.03	83.55	0.12	2352	2145
6-3	16.34	1.22	81.05	0.22	3180	2941
Sum	100.00					
Average		1.01	83.08	0.53	2571	2359

The largest share of grains was represented by the 20-10 mm size class (35.73%), while the smallest was in the 6-3 mm class (16.34%). The ash content was more than four times higher than in the combustible product, ranging from 81.05% to 84.19%, with an average value of 83.08%. The sulphur content in the waste sample varied from 0.12% (for the 10-6 mm size class) to 0.81% (for the 20-10 mm), with an average of 0.53%. The average calorific value was nearly 11 times lower than that of the combustible product, amounting to 2359 kJ/kg.

1.2.2. Results of density-qualitative analysis

Tables 11 - 13 (for the carbon-bearing product) and Tables 14 - 16 (for the mineral product) present the results of density-qualitative analyses for selected grain size classes.

Combustible product

Table 11 Density-qualitative composition of the carbon-bearing product in grain class 30-10 mm.

Density fraction	Share	Moisture content, W^a	Ash content, A^a	Sulphur content, S^a	Heat of combustion, Q_s^a	Calorific value, Q_i^a
g/cm^3	%	%	%	%	kJ/kg	kJ/kg
<1.5	71.97	1.71	9.61	0.87	29866	28778
1.5-1.8	22.85	1.77	31.27	0.62	21379	20545
>1.8	5.18	1.33	62.28	1.71	8895	8433
Sum	100.00					
Average		1.70	17.29	0.85	26840	25842

Table 12 Density-qualitative composition of the carbon-bearing product in grain class 10-3 mm.

Density fraction	Share	Moisture content, W^a	Ash content, A^a	Sulphur content, S^a	Heat of combustion, Q_s^a	Calorific value, Q_i^a
g/cm³	%	%	%	%	kJ/kg	kJ/kg
<1.5	66.69	1.76	8.62	0.72	30128	29027
1.5-1.8	15.37	1.78	38.15	0.72	19370	18618
>1.8	17.94	1.43	70.58	0.58	6614	6248
Sum	100.00					
Average		1.70	24.29	0.69	24255	23340

Table 13 Density-qualitative composition of the carbon-bearing product in grain class 30-3 mm.

Density fraction	Share	Moisture content, W^a	Ash content, A^a	Sulphur content, S^a	Heat of combustion, Q_s^a	Calorific value, Q_i^a
g/cm³	%	%	%	%	kJ/kg	kJ/kg
<1.5	70.54	1.72	9.34	0.82	29937	28845
1.5-1.8	20.82	1.77	33.14	0.65	20834	20023
>1.8	8.64	1.36	64.53	1.40	8277	7841
Sum	100.00					
Average		0.84	19.06	0.84	26170	25194

In the analysed material, the grain size classes 30-10 mm and 10-3 mm showed a predominant share of combustible fractions (<1.8 g/cm³), amounting to 94.82% and 82.06%, respectively. The share of fractions >1.8 g/cm³ was noticeably higher for the 10-3 mm grain size class (17.94%). The average ash content in the analysed classes 30-10 mm, 10-3 mm, and overall 30-3 mm was 17.29%, 24.29%, and 19.06%, respectively. The highest sulphur content was observed in the fraction with a density >1.8 g/cm³ for the 30-10 mm grain size class. The average sulphur content for the 30-3 mm class was 0.84%. The calorific value was slightly higher for the 30-10 mm class (25842 kJ/kg) compared to the 10-3 mm class (23340 kJ/kg).

Mineral product

Table 14 Density-qualitative composition of the mineral product sample in grain class 30-10 mm.

Density fraction	Share	Moisture content, W^a	Ash content, A^a	Sulphur content, S^a	Heat of combustion, Q_s^a	Calorific value, Q_i^a
g/cm³	%	%	%	%	kJ/kg	kJ/kg
<1.5	0.56	1.45	12.82	0.74	28802	27754
1.5-1.8	2.84	1.61	41.84	1.00	18565	17858
>1.8	96.60	0.90	84.58	0.72	1790	1597
Sum	100.00					
Average		0.92	82.97	0.73	2417	2204

Table 15 Density-qualitative composition of the mineral product in grain class 10-3 mm.

Density fraction	Share	Moisture content, W^a	Ash content, A^a	Sulphur content, S^a	Heat of combustion, Q_s^a	Calorific value, Q_i^a
g/cm³	%	%	%	%	kJ/kg	kJ/kg
<1.5	1.29	1.88	13.60	0.98	28661	27617
1.5-1.8	2.18	1.68	36.08	0.90	19796	19021
>1.8	96.53	1.18	84.27	0.15	1825	1624
Sum	100.00					
Average		1.20	82.31	0.18	2563	2339

Table 16 Density-qualitative composition of the mineral product in grain class 30-3 mm.

Density fraction	Share	Moisture content, W^a	Ash content, A^a	Sulphur content, S^a	Heat of combustion, Q_s^a	Calorific value, Q_i^a
g/cm³	%	%	%	%	kJ/kg	kJ/kg
<1.5	0.81	1.60	13.08	0.82	28753	27707
1.5-1.8	2.61	1.63	39.87	0.96	18987	18257
>1.8	96.58	1.00	84.47	0.53	1802	1606
Sum	100.00					
Average		1.02	82.73	0.54	2469	2252

In the analysed material, a small share of combustible fractions was observed, with material predominantly consisting of density fractions >1.8 g/cm³ (averaging 96.58%). The average ash content in the analysed grain size classes was 82.97% (30-10 mm class), 82.31% (10-3 mm class), and 82.73% for the entire analysed material (30-3 mm class). The sulphur content was significantly higher in the 30-10 mm grain size class

(average of 0.73%) compared to the 10-3 mm class, where it averaged 0.18%. The average sulphur content in the entire waste material was 0.54%. The waste material was characterized by a significantly lower average calorific value (2252 kJ/kg for the 30-3 mm class) compared to the carbon-bearing product, whose value was more than 11 times higher.

1.3. Karvina 2 product samples

The product samples were obtained from the jig separation of material collected from the Jan Karel heap, a and the sampling location is shown in Figure 3.

Figure 3 Places of collecting the sample Karviná 2 - 49.8509372N, 18.4916761E

1.3.1. Results of granulometric-qualitative analysis

In the grain size classes obtained from the granulometric analysis of the samples, the moisture content, ash content, sulphur content, calorific value, and heating value (in the analytical state) were determined. The analysis results for the carbon-bearing product are presented in Table 17, and for the mineral fraction in Table 18.

Table 17 Granulometric-qualitative composition of the carbon-bearing product.

Grain class	Share	Moisture content, W^a	Ash content, A^a	Sulphur content, S^a	Heat of combustion, Q_s^a	Calorific value, Q_i^a
mm	%	%	%	%	kJ/kg	kJ/kg
30-20	6.91	1.28	8.29	1.17	30826	29728
20-10	25.53	1.16	39.86	0.27	18872	18148
10-6	31.29	1.35	37.89	0.52	19190	18440
6-3	36.27	1.41	42.43	0.41	17911	17214
Sum	100.00					
Average		1.32	37.99	0.46	19449	18701

In the analysed material, the dominant grain size classes were 6-3 mm and 10-3 mm, which together accounted for over 67% of the total material. The smallest share was represented by the 30-20 mm grain size class (6.91%), which had the lowest ash content

of 8.29%, while also having the highest sulphur content at 1.17%. The average ash content for this material was 37.99%, sulphur content was 0.46%, and the calorific value was 18701 kJ/kg.

Table 18 Granulometric-qualitative composition of the mineral product.

Grain class	Share	Moisture content, W^a	Ash content, A^a	Sulphur content, S^a	Heat of combustion, Q_s^a	Calorific value, Q_i^a
mm	%	%	%	%	kJ/kg	kJ/kg
30-20	15.73	0.89	85.17	0.14	1662	1476
20-10	35.25	0.03	83.47	0.05	2098	1903
10-6	25.90	0.11	85.48	0.04	1512	1339
6-3	23.12	0.85	81.62	0.15	3150	2922
Sum	100.00					
Average		0.38	83.83	0.08	2121	1925

In the analysed material, the largest share, 35.25%, was represented by the 20-10 mm grain size class. Similar to the combustible product, the smallest share was in the 30-20 mm class, at 15.73%. The ash content, regardless of the grain size class, was above 80%, with an average of 83.83%. The average sulphur content was 0.08%, and

the average calorific value was more than 9 times lower than that of the carbon-bearing product, amounting to 1925 kJ/kg.

1.3.2. Results of density-qualitative analysis

Tables 19 - 21 (for the carbon-bearing product) and Tables 22 -24 (for the mineral product) present the results of density-qualitative analyses for selected grain size classes.

Combustible product

Table 19 Density-qualitative composition of the carbon-bearing product in grain class 30-10 mm.

Density fraction	Share	Moisture content, W^a	Ash content, A^a	Sulphur content, S^a	Heat of combustion, Q_s^a	Calorific value, Q_i^a
g/cm^3	%	%	%	%	kJ/kg	kJ/kg
<1.5	32.34	1.26	8.35	0.63	31357	30259
1.5-1.8	52.50	1.17	39.30	0.51	18697	17966
>1.8	15.15	0.75	61.38	0.34	10726	10261
Sum	100.00					
Average		1.14	32.63	0.52	21584	20775

Table 20 Density-qualitative composition of the carbon-bearing product in grain class 10-3 mm.

Density fraction	Share	Moisture content, W^a	Ash content, A^a	Sulphur content, S^a	Heat of combustion, Q_s^a	Calorific value, Q_i^a
g/cm^3	%	%	%	%	kJ/kg	kJ/kg
<1.5	30.81	1.36	8.69	0.46	30815	29720
1.5-1.8	32.35	1.18	40.67	0.44	18594	17879
>1.8	36.84	1.12	64.84	0.26	8972	8543
Sum	100.00					
Average		1.21	39.72	0.38	18815	18088

Table 21 Density-qualitative composition of the carbon-bearing product in grain class 30-3 mm.

Density fraction	Share	Moisture content, W^a	Ash content, A^a	Sulphur content, S^a	Heat of combustion, Q_s^a	Calorific value, Q_i^a
g/cm³	%	%	%	%	kJ/kg	kJ/kg
<1.5	31.31	1.33	8.58	0.51	30991	29895
1.5-1.8	38.89	1.18	40.23	0.46	18627	17907
>1.8	29.80	1.00	63.72	0.29	9541	9100
Sum	100.00					
Average		1.17	37.32	0.43	19790	19036

The analysed particle size classes varied significantly in terms of the share of intermediate-density fractions (1.5-1.8 g/cm³) and waste fractions (>1.8 g/cm³). In the 30-10 mm particle size class, the share of these fractions was 52.50% and 15.15%, respectively, whereas the 10-3 mm class had a much lower proportion of intermediate-density fractions, at 32.25%.

The average ash contents in the analysed size classes of 30-10 mm, 10-3 mm, and cumulatively 30-3 mm were 32.63%, 39.72%, and 37.32%, respectively. A higher average sulphur content of 0.52% was observed in the 30-10 mm particle size class. The average sulphur content in the 30-3 mm class was 0.43%. The average calorific value was slightly higher for the 30-10 mm class (20775 kJ/kg) than for the 10-3 mm class (18088 kJ/kg). However, these were the lowest values among all the analysed the carbon-bearing product.

Mineral product

Table 22 Density-qualitative composition of the mineral product in grain class 30-10 mm.

Density fraction	Share	Moisture content, W^a	Ash content, A^a	Sulphur content, S^a	Heat of combustion, Q_s^a	Calorific value, Q_i^a
g/cm³	%	%	%	%	kJ/kg	kJ/kg
<1.5	0.08	1.32	13.20	0.41	29461	28420
1.5-1.8	1.87	0.61	43.50	0.34	17216	16541
>1.8	98.05	0.78	85.75	0.08	1375	1197
Sum	100.00					
Average		0.78	84.90	0.09	1694	1506

Table 23 Density-qualitative composition of the mineral product in grain class 10-3 mm.

Density fraction	Share	Moisture content, W^a	Ash content, A^a	Sulphur content, S^a	Heat of combustion, Q_s^a	Calorific value, Q_i^a
g/cm³	%	%	%	%	kJ/kg	kJ/kg
<1.5	0.32	1.24	10.12	0.48	30619	29542
1.5-1.8	1.88	1.22	37.72	0.40	19763	19013
>1.8	97.80	0.88	84.49	0.09	1912	1718
Sum	100.00					
Average		0.89	83.37	0.10	2339	2132

Table 24 Density-qualitative composition of the mineral product in grain class 30-3 mm.

Density fraction	Share	Moisture content, W^a	Ash content, A^a	Sulphur content, S^a	Heat of combustion, Q_s^a	Calorific value, Q_i^a
g/cm³	%	%	%	%	kJ/kg	kJ/kg
<1.5	0.20	1.28	11.69	0.44	30028	28970
1.5-1.8	1.87	0.91	40.66	0.37	18464	17753
>1.8	97.93	0.83	85.13	0.08	1638	1452
Sum	100.00					
Average		0.83	84.15	0.09	2010	1813

The analysed material contained a very small share of combustible fractions (on average 2.07%) – the material with a density fraction >1.8 g/cm³ was the main component (on average 97.93%). The ash content in the 30-3 mm particle size class was 84.15%. The sulphur content was comparable for the 30-10 mm and 10-3 mm classes, with an average of 0.09%, which is more than 4.5 times lower than in the case of the carbon-bearing product. The average calorific value was higher in the 10-3 mm particle size class (2132 kJ/kg) than in the 30-10 mm class (1506 kJ/kg). The mineral product had an over 10 times lower average calorific value (1813 kJ/kg for the 30-3 mm particle size class) compared to the carbon-bearing product.

2. Physicochemical analyses and mechanical property tests of the separation products

2.1. Mineral product research

The Table 25 presents the sample indexes for testing prepared as part of the task 3.2.

Table 25 The samples transferred to the GIG for examination in WP3.

Sample	ID
Mineral jig product Haldex 1 – mineral fraction from Haldex 1 waste heap	H1/m
Mineral jig product Haldex 2 – mineral fraction from Haldex 2 waste heap	H2/m
Mineral jig product Karvina 2 – mineral fraction from Karvina 2 waste heap	K2/m
Mineral fraction HALDEX – Material for calcination	H/m
Carbon-bearing jig product Haldex 1 – coal fraction from Haldex 1 waste heap	H1/c
Carbon-bearing jig product Haldex 2 – coal fraction from Haldex 2 waste heap	H2/c
Carbon-bearing jig product Karvina 2 – coal fraction from Karvina 2 waste heap	K2/c
Carbon-bearing fraction HALDEX – Material for gasification	H/c
Fly ash from Jaworzno (Poland) Power Plant	FA

Research on the mineral fraction included determining its structure and mechanical properties. As part of Task 3.2, the following tests were performed:

- Crushing resistance of aggregates (Los Angeles Index),
- Wear resistance of aggregates (micro-Deval),
- Water absorption,
- Frost resistance,
- SEM/EDS analysis.

Additionally, for the mineral fraction HALDEX (H/m) and fly ash (FA), the mineral composition was analysed, and physicochemical tests were also conducted for the H/m sample. At this stage of the research, a grain size composition analysis of the samples was carried out. This analysis was performed using the 'wet' sieving method with square sieves measuring 0.5 m on each side. The sieves had square openings of

sizes 32 mm, 16 mm, 8 mm, and 4 mm. The results of the grain size composition analysis are presented in Figure 4.

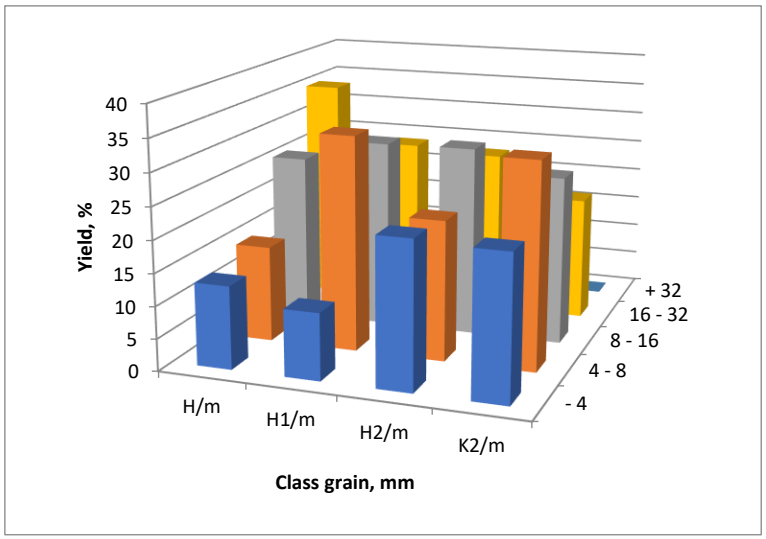

Figure 4 Grain size composition analysis of the 4 mineral fraction samples.

Grains sized 4 - 8mm and 8 - 16mm dominate in most of the samples, which may indicate that the samples are well balanced in terms of medium-sized grains. The samples contain relatively few large grains (>32mm), which is typical for materials intended for applications requiring finer components (e.g., concrete mixes).

2.1.1. Determination of the crushing resistance of aggregates via the Los Angeles method

In the first stage, the samples were separated (by the wet method) into 5 fractions: > 32 mm; 32-16 mm; 16-8 mm; 8-4 mm; and < 4 mm. For the determination of crushing resistance via the Los Angeles method, according to the standard PN-EN 1097-2, the 16-8mm fraction was washed out wetly from the waste, conforming to the standard requirements, yielding a fraction with a grain size of 14-10 mm.

The Los Angeles method for determining crushing resistance involves crushing the material in a rotating steel drum containing 11 steel balls with a diameter of 47 mm and a total mass of 4690±860 g.

Course of the test and determination of the Los Angeles (LA) index. From the prepared fraction of 14-10 mm, approximately 15 kg was taken and reduced by quartering to a mass of 5000±5 g. After drying to a constant mass, the collected waste was placed in the Los Angeles drum along with the steel balls, and the device was started. The drum rotational speed ranged from 31 to 33 rpm, and the number of drum revolutions was 500. After the drum stopped, the material was removed from the drum and washed with water on a 1.6mm sieve. The residue above 1.6mm was dried to a constant mass and weighed.

The Los Angeles (LA) index was calculated via the following formula:

$$\mathbf{LA = (5000 - m)/50}$$

where, m - mass of material with a grain size above 1.6 mm.

Table 26 presents the results of the LA index determination for the analysed waste.

Table 26 Crushing resistance determined by the Los Angeles method.

Sample	LA (%)
H1/m	40.3
H2/m	45.2
K2/m	31.2
H/m	29.7

So, in the context of PN-EN 1097-2, where the LA value is used as an indicator of the durability of aggregates, the acceptable limits for LA values are generally:

- LA ≤ 30: Considered suitable for high-quality materials, such as aggregates used in road pavements, where high durability is required.
- LA > 30: Indicates lower-quality aggregates, which may not meet the requirements for applications that demand high abrasion resistance (e.g., road pavements).

Sample H1/m: This result is above 30, indicating that the aggregate in this sample has lower abrasion resistance and might not meet the high-quality material requirements for road construction or similar uses.

Sample Haldex H2/m: 45.2% – This result is also high (above 30), suggesting that this sample has even lower resistance to abrasion and might not be suitable for use in applications requiring high abrasion resistance.
Sample Karvina K2/m: 31.2% – The result of 31.2% is slightly above 30, but still in an acceptable range for certain uses. Further verification may be needed depending on the material's intended application.
Sample Haldex H/m: 29.7% – This result is below 30, meaning it meets the standard for abrasion resistance and would be suitable for many construction applications.
H1/m and H2/m have results of 40.3% and 45.2%, which exceed the threshold of 30 and may suggest the need for further investigation into the suitability of these materials for construction purposes, particularly in road surfaces.
K2/m (31.2%) is just above 30 but might still be acceptable for certain uses, especially if the material is not intended for the most demanding applications.
H/m (29.7%) meets the standard and can be considered suitable for use in high-quality construction materials.

2.1.2. Determination of the abrasion resistance of aggregates via the micro-Deval method

The abrasion resistance of the aggregates was determined via the micro-Deval (wet method) according to the standard PN-EN 1097-1. Grain classes of 4-8 mm were used for the tests. In accordance with the standard, the particle size distribution of each sample was checked through an intermediate sieve with an opening size of 6.3 mm. The samples were rinsed in water and dried to a constant mass at a temperature of 110°C. Samples weighing 500 g each were placed in the device's container, and 2.8 dm^3 of water was added. Simultaneously, tests were conducted on 2 samples of each waste type. Covers were placed on each container, and they were positioned on the rollers of the coefficient determination device. The device rotated the containers at a speed of 100 rpm. The specified number of revolutions was 12,000±10 revolutions. After the device was stopped, the containers were opened, and their contents were transferred to a protective sieve with an opening size of 10 mm. The protective sieve

was placed on another sieve with an opening size of 1.6 mm. The material with the steel balls was rinsed on sieves under a stream of clean water. The balls were carefully separated from the material on the protective sieve. The remaining mineral material was transferred to a sieve with an opening size of 1.6 mm and rinsed with water. The material remaining on the sieve was transferred to a tray, dried at a temperature of 100°C, and weighed. The micro-Deval coefficient was calculated for each sample using the formula:

$$Mde = \frac{500 - m}{5}$$

where,

Mde - is micro-Deval coefficient (determined in the wet state),

M - is mass of the fraction retained on the 1.6 mm sieve, in g.

Using the values obtained for 2 results for each sample, the average values were calculated, rounded to the nearest whole number, and compiled in Table 27.

Table 27 The abrasion resistance determined via the micro-Deval method.

Sample	Micro-Deval (%)	Average (%)
H1/m	67.66	69
H1/m	69.50	
H/m	77.26	77
H/m	76.56	
H2/m	77.86	78
H2/m	78.36	
K2/m	58.88	60
K2/m	60.84	

According to PN-EN 1097-1, for aggregates used in road construction and concrete materials:

The maximum permissible value for the Micro-Deval result is typically around 20% for aggregates for asphalt or concrete. However, allowable limits can vary depending on the type of aggregate and its intended use. Samples with results above 20%

indicate lower resistance to abrasion, which may mean the material does not meet the requirements for its durability and resistance to wear in more demanding construction applications.

Mineral jig product Haldex 1 – mineral fraction from Haldex 1 waste heap (H1/m):

Micro-Deval results are 67.66% and 69.50%, with an average of 69%.

Analysis: These results are significantly higher than the typical limits of PN-EN 1097-1 for aggregates used in road or concrete construction. Acceptable values for road construction aggregates are usually below 20%, so 69% indicates very poor resistance to abrasion. This material is not suitable for use in applications requiring high durability (e.g., road surfaces).

Mineral fraction HALDEX:

Micro-Deval results are 77.26% and 76.56%, with an average of 77%.

Analysis: Similar to Haldex 1, these results also significantly exceed the allowable limits of PN-EN 1097-1. 77% indicates a very high mass loss, meaning this material also has poor abrasion resistance. This material is not suitable for road or concrete applications either.

Mineral jig product Haldex 2 – mineral fraction from Haldex 1 waste heap (H2/m):

Micro-Deval results are 77.86% and 78.36%, with an average of 78%.

Analysis: The results for Haldex 2 are the highest among all the samples, but still far exceed the permissible limits of PN-EN 1097-1. 78% indicates very poor resistance to abrasion and the material is unsuitable for road construction or similar high-durability applications.

Mineral jig product Karvina 2 – mineral fraction from Karvina 2 waste heap (HK/m):

Micro-Deval results are 58.88% and 60.84%, with an average of 60%.

Analysis: Although 60% is lower than the results for the Haldex samples, it still greatly exceeds the allowable values of PN-EN 1097-1 for high-abrasion-resistant aggregates like those used in road or concrete construction.

2.1.2. Water Absorption

The determination of water absorption was performed in accordance with the standard PN-EN 1097-6. The samples were prepared from homogeneous material with a mass selected according to the grain size of the tested material (Table 28).

Table 28 The standard specifies the minimum sample mass required for different grain size classes.

Grain size class (mm)	Minimum sample mass (g)
Above 8 mm	1000
Above 16 mm	2000
Above 32 mm	5000

The samples were placed in baskets and submerged in water to a height of approximately 5 cm above the level of the tested waste. The material was then left in the water until the samples were fully saturated. After a given time, the samples were removed, dried with an absorbent cloth, and weighed. The next step in the test was drying to a constant mass by placing the samples in an oven at a temperature of approximately 110°C for 24 hours. After being removed from the oven, the samples were weighed.

The water absorption of the aggregate is determined via the following formula:

$$W_A = \frac{m_1 - m}{m} \cdot 100\%$$

where, m - is the mass of the sample dried to a constant weight, in grams, and m1 is the mass of the sample fully saturated with water, in grams.

Figure 5 presents the results of the water absorption index determination.

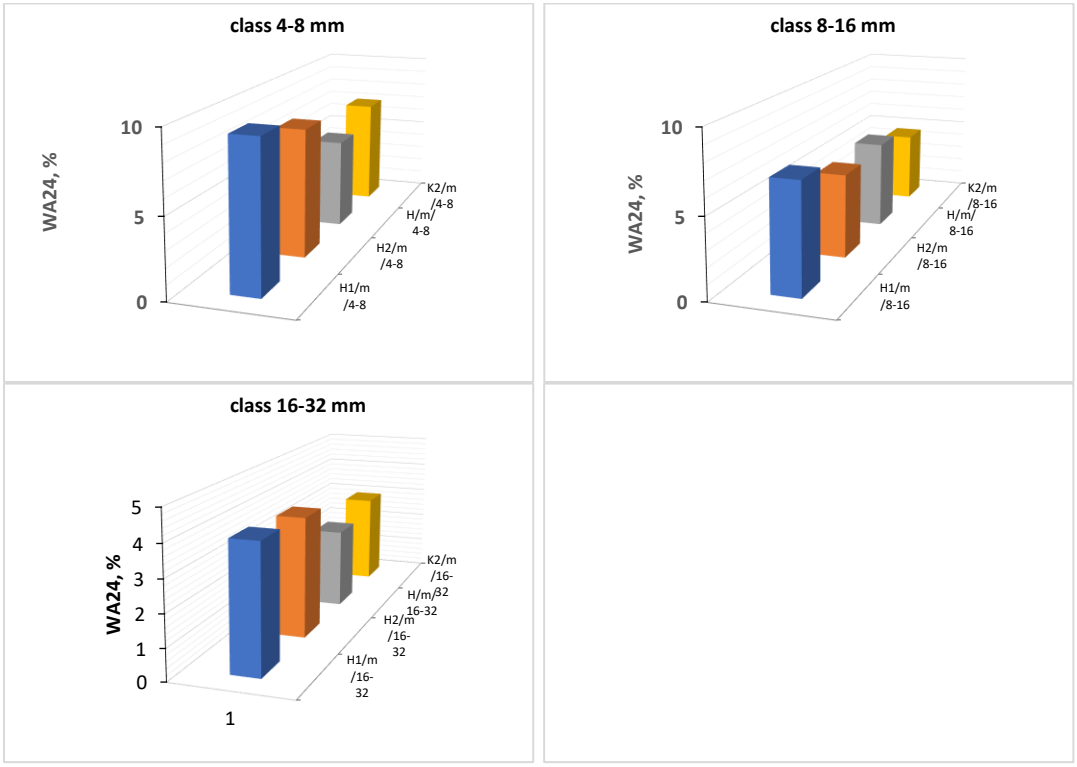

Figure 5 Water absorption of waste in grain size classes

The analysis of water absorption for samples in different grain size classes (4-8 mm, 8-16 mm, 16-32 mm) shows varying levels of water absorption, indicating differences in porosity and material structure:

Class 4-8 mm: The H1/m/4-8 sample has the highest water absorption (9%), and H2/m/4-8 has slightly lower absorption (8%). H/m/4-8 has the lowest absorption (5-6%), and K2/m/4-8 falls in the medium range (7%). According to the European standard, water absorption should not exceed 1% to guarantee frost resistance, so none of the samples in this class meet this requirement.

Class 8-16 mm: Similar to the 4-8 mm class, the H1/m/4-8 sample has the highest water absorption (9%), and the K2/m/4-8 sample falls in the medium range (7%).

Class 16-32 mm: The H1/m/s16-32 sample has the highest water absorption (4%), and H2/m/s16-32 (3.7%) shows slightly lower absorption. The other samples in this class have progressively lower water absorption, indicating moderate water absorption.

All samples have higher water absorption than the required 1%, meaning they do not meet the European standard for frost resistance.

2.1.3. Frost Resistance

Frost resistance tests were conducted according to the standard PN-EN 1367-1. The tests were performed for the following grain size classes: 4-8 mm, 8-16 mm, and 16-32 mm.

Figure 6 Frost resistance test – preparing samples

The test consisted of the following stages:

1. The waste sample taken for testing was dried at a temperature of (110±5) °C to a constant mass.
2. The waste sample (M1) was placed in a metal can with the following dimensions: outer diameter: 130 mm, outer height: 200 mm. The minimum mass of the sample for testing is specified in Table 5.
3. The waste was submerged in distilled water (10mm above the upper layer of waste) and left for 24 hours at a temperature of (20±5) °C.
4. The can was covered and placed in a climatic chamber.
5. The following temperature change cycle was implemented as a function of time:
    - the temperature was changed from (20 ± 5) °C to a temperature ranging from (0 to -1)°C in (150 ± 60) min and maintained at the set temperature for (210±90) min.,

- the temperature was changed from (0 to -1) °C to (-17.5 ± 2.5) °C in (180 ± 60) min and maintained at the set temperature for a minimum of 240 min.,
- the can was removed from the chamber and thawed by immersion in water,
- the cycle lasted a total of 24 hours.

6. Steps 4-5 were repeated 10 times.

After 10 cycles, the sample was sieved through a sieve with sizes specified in Table 29. The residue on the sieve was dried at a temperature of (110±5)°C and weighed (M2). The coefficient F, which determines the percentage loss of mass of a sample after 10 freeze–thaw cycles, was calculated via the following formula:

$$\mathbf{F} = \frac{\mathbf{M1} - \mathbf{M2}}{\mathbf{M1}} * \mathbf{100}$$

Table 29 Mass of waste required for test.

Grain size class (mm)	Minimum sample mass (g)	Sieve size (mm)
4 - 8 mm	1000	2
8 - 16 mm	2000	4
16 - 32 mm	4000	8

Figure 7 presents the results of the frost resistance determination.

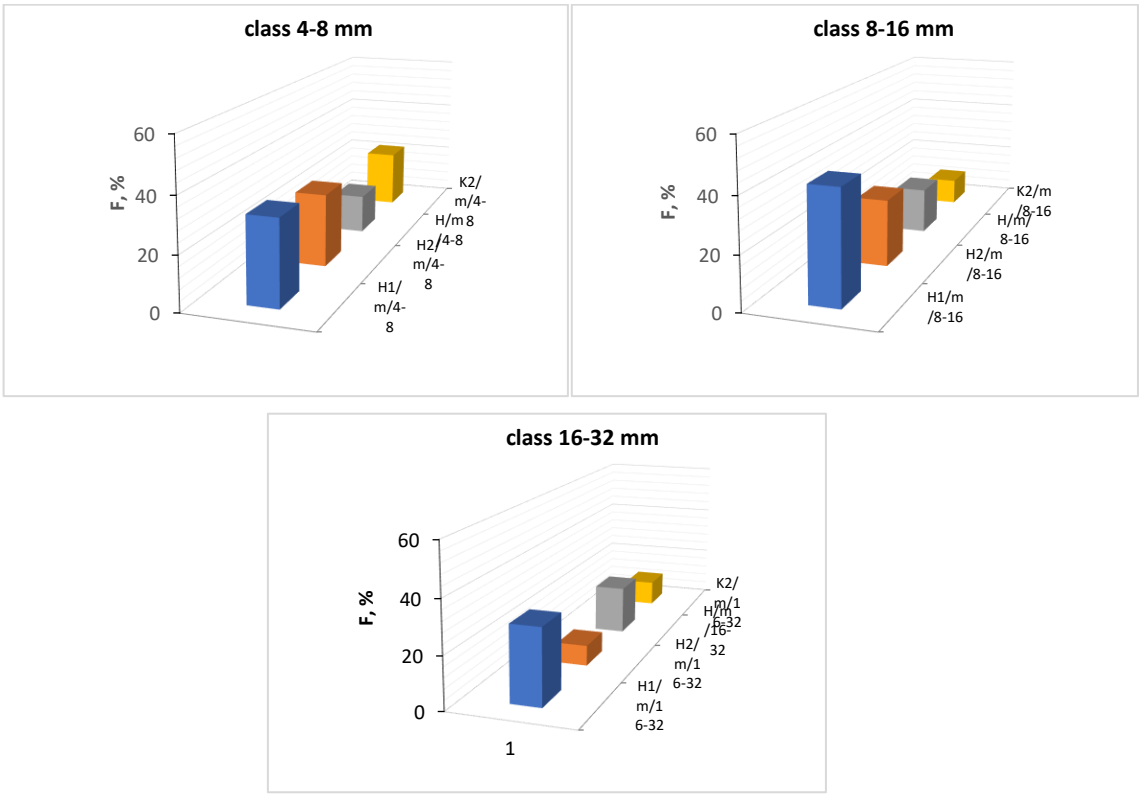

Figure 7 Frost resistance of waste in grain size classes

In the analysis of frost resistance of various samples in three grain size classes (8-16 mm, 16-32 mm, and 4-8 mm), the results indicate different levels of frost resistance for the materials:

Class 4-8 mm:

H/m/4-8 mm shows the best frost resistance (14.6% mass loss).

K2/m/4-8 mm has average frost resistance (21.8% mass loss).

H1/m/4-8 mm and H2/m/4-8 mm have higher mass loss (27.2% and 31.7%), indicating poorer frost resistance.

Class 8-16 mm:

K2/m/8-16 mm offers the best frost resistance (9.9% mass loss).

H/m/8-16 mm (17.2%) has medium frost resistance.

H2/m/8-16 mm (25.1%) and H1/m/8-16 mm (42.0%) have lower frost resistance, with H1 being the least resistant.

Class 16-32 mm:

H2/m/16-32 mm has minimal mass loss (7.9%), indicating very high frost resistance.

K2/m/16-32 mm (10.0%) also has good frost resistance, but slightly lower than H2.

H/m/16-32 mm (18.8%) is a material with medium frost resistance.

H1/m/16-32 mm (29.1%) is the least frost-resistant material.

Depending on the frost resistance requirements of the project, K2/m/8-16 mm and H2/m/16-32 mm show the best performance, while H1/m/8-16 mm and H1/m/16-32 mm should be avoided in more demanding conditions.

2.2. SEM/EDS Analysis

A scanning electron microscope with variable vacuum (SEM-SU3500 from Hitachi) was used to observe the surface structure of the samples, in conjunction with an energy dispersive X-ray spectrometer (EDS) UltraDry from Thermo Scientific. The studies were conducted in variable vacuum mode with an accelerating voltage of 15 keV.

For the preparation, several BSE (backscattered electron) images were recorded, showing the morphology and size of the waste particles and the diversity of their chemical composition. For the selected particles, EDS spectra were recorded, illustrating their chemical composition. A series of microanalyses were performed on the samples, including from several to dozens of measurements of their chemical composition to determine the presence of individual elements (Figure 8). The final result is the average of the measurements of the chemical composition in the microarea.

The analyses showed that in the H1/m, H2/m, H/m, and K2/m samples, Si is the dominant component, with an average content ranging from 15.95 to 21.64 wt.%, followed by Fe with an average from 10.50 to 13.49 wt.%, and Al with an average from

8.11 to 10.42 wt.%. In the H1/m sample, Ba was also observed, with an average content of 1.37 wt.%. Other chemical constituents such as Na, Mg, P, S, K, Ca, Cl, Ti, Cr, Mn, Co, Ni, Zn, Pb, Cu, Mo were present in several percent. Rare earth elements such as Pr, Ce, Nd, and Sm were also occasionally found in the particles.

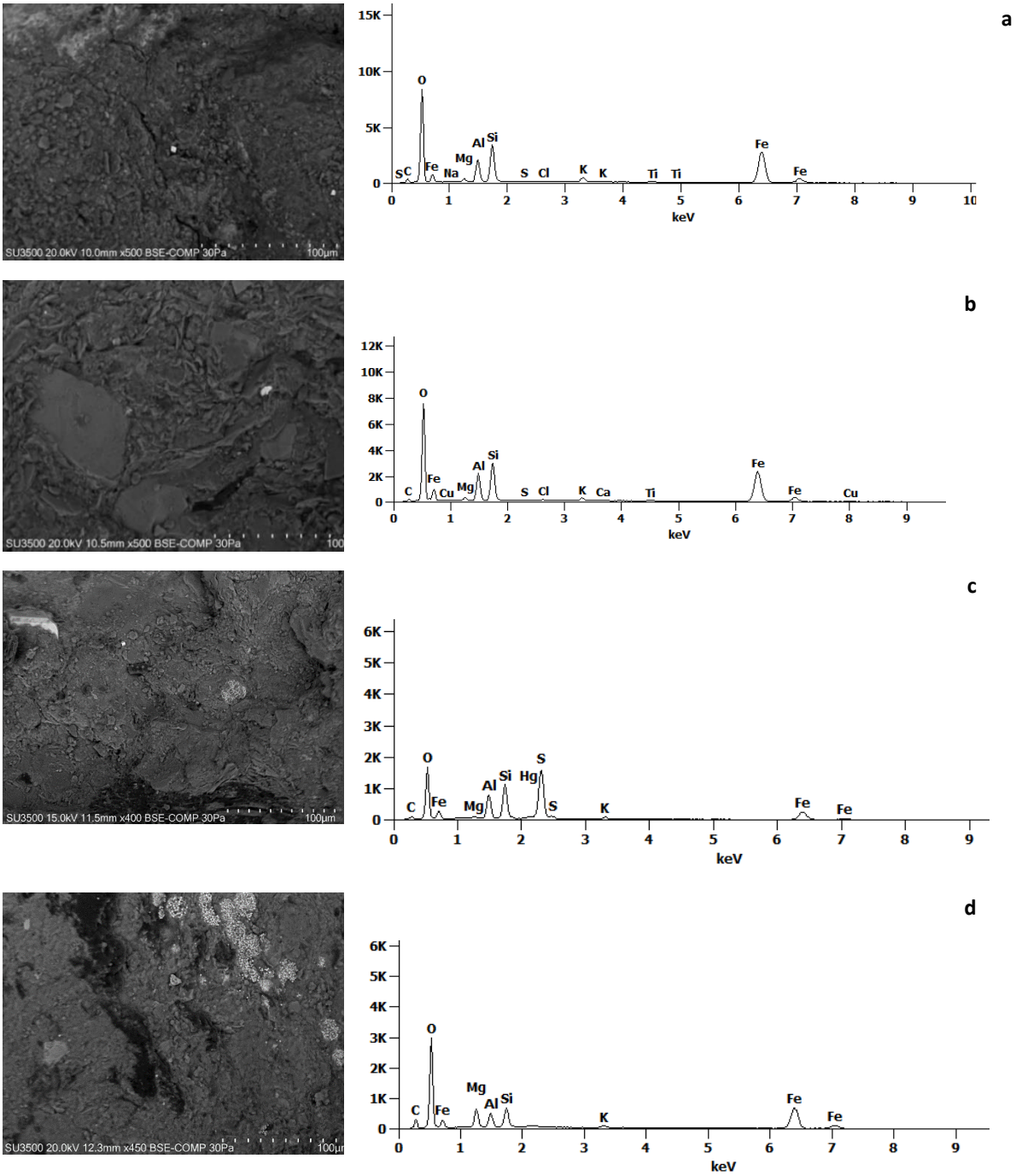

Figure 8 Morphology of the sample and chemical composition SEM EDS of the samples: a) H1/m, b) H2/m, c) H/m, and d) K2/m.

2.3. Respiratory Activity of Microorganisms (AT4)

Respiratory activity is a parameter used to determine the biological stability/activity of waste. Considering the measurement results for the input sample (not separated into mineral and carbon fractions) within WP2 (AT4 below 4 mg O2/g), no studies were conducted in WP3.

2.4. Proximate, ultimate, and calorific value analyses

After separation, the samples were divided into two fractions: one enriched in flammable parts (coal fraction) and the other enriched in mineral parts (mineral fraction). Table 30 and 31 show the proximate and ultimate analysis results for the coal and mineral fractions, respectively.

Table 30 Proximate and ultimate analysis of coal fraction.

Type of research / Research method	Symbol	Unit	Carbon-bearing jig product Haldex1	Carbon-bearing jig product Haldex2	Carbon-bearing jig product Karvina2	HALDEX-material for gasification
Moisture content (as received basis) PN-ISO 589:2006 Method B1	M_{ar}	%	2.0	2.3	1.7	3.8
Moisture content (as determined basis) PN-ISO 11722:2009	M_{ad}	%	1.4	1.6	1.3	1.6
Ash content (as determined basis) PN-ISO 1171:2002	A_{ad}	%	22.5	21.7	39.9	16.0
Ash content (as received) PN-ISO 1171:2002	A_{ar}	%	22.4	21.5	39.7	15.6
Ash content (dry basis) PN-ISO 1171:2002	A_d	%	22.8	22.1	40.4	16.3
Volatile matter content (as determined basis) ISO 562:2010	V_{ad}	%	26.91	27.24	20.75	28.58
Volatile matter content (dry basis) ISO 562:2010	V_d	%	27.29	27.68	21.02	29.04

Volatile matter content (dry ash free basis) ISO 562:2010	V_{daf}	%	35.36	35.51	35.29	34.68
Heat of combustion (as determined basis) PN-ISO 1928:2020-05	$Q_{v, gr, ad}$	J/g	25 640	25 750	18 860	27 895
Heat of combustion (dry basis) PN-ISO 1928:2020-05	$Q_{v, gr, d}$	J/g	26 000	26 170	19 110	28 350
Calorific value (as determined basis) PN-ISO 1928:2020-05	$Q_{p, net, ad}$	J/g	24 750	24 830	18 190	26 920
Calorific value (as received basis) PN-ISO 1928:2020-05	$Q_{p, net, ar}$	J/g	24 580	24 630	18 110	26 260
Total sulfur content (as determined basis) ISO 19579:2006	$S_{T, ad}$	%	0.73	0.77	0.31	0.72
Total sulfur content (as received basis) ISO 19579:2006	$S_{T, ar}$	%	0.73	0.76	0.31	0.70
Total sulfur content (dry basis) ISO 19579:2006	$S_{T, d}$	%	0.74	0.78	0.31	0.73
Total carbon content (as determined basis) ISO 29541:2010	C_{ad}	%	63.5	62.9	47.7	68.3
Total carbon content (as received basis) ISO 29541:2010	C_{ar}	%	63.1	62.5	47.5	66.8
Total carbon content (dry basis) ISO 29541:2010	C_{d}	%	64.4	63.9	48.3	69.4
Total hydrogen content (as determined basis) ISO 29541:2010	H_{ad}	%	4.17	4.33	3.14	4.57
Total hydrogen content (dry basis) ISO 29541:2010	H_{d}	%	4.07	4.22	3.03	4.46
Nitrogen content (as determined basis) ISO 29541:2010	N_{ad}	%	1.01	1.04	0.73	1.01
Nitrogen content (dry basis) ISO 29541:2010	N_{d}	%	1.02	1.06	0.74	1.03
Chlorine content (as determined basis) PN-G-04534:1999	Cl^{a}	%	0.054	0.054	0.036	0.081
Chlorine content (dry basis) PN-G-04534:1999	Cl^{d}	%	0.055	0.055	0.036	0.082

Table 31 Proximate and ultimate analysis of mineral fraction.

Type of research / Research method	Symbol	Unit	Mineral jig product Haldex 1	Mineral jig product Haldex 2	Mineral jig product Karvina 2	HALDEX material for calcination
Moisture content (as received basis) PN-ISO 589:2006 Method B1	M_{ar}	%	0.7	0.8	1.1	1.3
Moisture content (as determined basis) PN-ISO 11722:2009	M_{ad}	%	1.0	0.8	0.9	0.9
Ash content (as determined basis) PN-ISO 1171:2002	A_{ad}	%	83.4	82.1	83.5	88.0
Ash content (as received) PN-ISO 1171:2002	A_{ar}	%	83.7	82.1	83.3	87.6
Ash content (dry basis) PN-ISO 1171:2002	A_d	%	84.2	82.8	84.3	88.8
Volatile matter content (as determined basis) ISO 562:2010	V_{ad}	%	9.99	10.51	10.30	8.19
Volatile matter content (dry basis) ISO 562:2010	V_d	%	10.09	10.59	10.39	8.26
Volatile matter content (dry ash free basis) ISO 562:2010	V_{daf}	%	64.04	61.46	66.03	73.78
Heat of combustion (as determined basis) PN-ISO 1928:2020-05	$Q_{v, gr, ad}$	J/g	2 460	3 040	2 240	1210
Heat of combustion (dry basis) PN-ISO 1928:2020-05	$Q_{v, gr, d}$	J/g	2 480	3 060	2 260	1220
Calorific value (as determined basis) PN-ISO 1928:2020-05	$Q_{p, net, ad}$	J/g	2 180	2 760	1 970	990
Calorific value (as received basis) PN-ISO 1928:2020-05	$Q_{p, net, ar}$	J/g	2 200	2 760	1 960	970
Total sulfur content (as determined basis) ISO 19579:2006	$S_{T, ad}$	%	0.63	0.59	0.06	0.10
Total sulfur content (as received basis) ISO 19579:2006	$S_{T, ar}$	%	0.63	0.59	0.06	0.10
Total sulfur content (dry basis) ISO 19579:2006	$S_{T, d}$	%	0.64	0.59	0.06	0.10
Total carbon content (as determined basis) ISO 29541:2010	C_{ad}	%	8.1	9.6	7.9	4.9

Total carbon content (as received basis) ISO 29541:2010	C_{ar}	%	8.1	9.6	7.9	4.9
Total carbon content (dry basis) ISO 29541:2010	C_d	%	8.2	9.7	8.0	4.9
Total hydrogen content (as determined basis) ISO 29541:2010	H_{ad}	%	1.26	1.28	1.25	1.02
Total hydrogen content (dry basis) ISO 29541:2010	H_d	%	1.16	1.20	1.16	0.93
Nitrogen content (as determined basis) ISO 29541:2010	N_{ad}	%	0.18	0.19	0.16	0.09
Nitrogen content (dry basis) ISO 29541:2010	N_d	%	0.18	0.19	0.16	0.09
Chlorine content (as determined basis) PN-G-04534:1999	Cl^a	%	0.018	0.018	0.009	0.041
Chlorine content (dry basis) PN-G-04534:1999[1)]	Cl^d	%	0.018	0.018	0.009	0.041

Samples enriched in flammable parts (coal fraction) are characterized by a relatively high calorific value as received basis (except for the Karvina2 sample), which exceed 24 MJ/kg. These samples are characterized by a mineral content not exceeding 23%, except for the aforementioned Karvina2 sample (Table 30). The lower calorific value of the Karvina2 sample and increased ash content as received basis (i.e. 39.7%) in relation to the other samples is probably caused by the occurrence of reduced efficiency of the flammable part separation in the case of this sample. Very large differences between samples enriched in flammable parts (Table 30) and samples enriched in mineral parts (Table 31) were noted. Calorific value, heat of combustion and the content of elemental carbon - fixed carbon (FC=100-Vr-Ar-Mr) indicate high efficiency of the separation process. Defining the separation efficiency in terms of carbon content (equation (1) and fixed carbon content (equation (2), the following values were obtained for the individual samples (Table 32). As can be seen from the values presented in the Table 32, in the case of the Haldex1 and Karvina2 samples, the efficiency was above 48%. In the case of the Haldex2 sample, this efficiency is clearly lower and is below 28%. Such a low value of η_C was caused by the relatively low carbon content in the raw samples (i.e. 12.7 wt.% as received basis) and

the relatively high carbon content in the mineral fraction after separation (i.e. 9.6 wt.% as received basis). A similar trend was observed for η_{FC}. The bound carbon content in the case of the raw Haldex2 sample was "only" 9.1 wt.%. (which in turn was caused by a relatively high ash content as received basis, i.e. 77.3% by weight), while in the case of the mineral part after separation, the FC content was "as much as" 6.6% by weight.

$$\eta_C = \left(1 - \frac{C_{r,mineral-jig}}{C_{r,raw\ sample}}\right) \times 100\% \quad (1)$$

$$\eta_{FC} = \left(1 - \frac{FC_{r,mineral-jig}}{FC_{r,raw\ sample}}\right) \times 100\% \quad (2)$$

Table 32 Separation efficiency due to carbon content, ηC, % (equation (1)) and fixed carbon content, ηFC, % (equation (2)).

Sample	Haldex1	Haldex2	Karvina 2
ηC, %	54.2	24.4	48.4
ηFC, %	57.3	27.6	54.0

Samples separated using the jig beneficiation system (developing by KOMAG), such as Carbon-bearing jig product Haldex1 and Haldex2, were enriched with combustible material (carbon fraction), exhibiting high calorific values in working conditions (>24 MJ/kg) and promising volatile matter content (V_{daf} >34%). Sulfur content varied significantly across samples. The Karvina2 sample demonstrated notably lower sulfur levels in both coal (S_t = 0.31 wt.%) and mineral fractions (S_t = 0.06 wt.%) compared to the other samples (S_T = 0.73–0.77 wt.% in coal and S_T = 0.59–0.63 wt.% in minerals). Higher sulfur levels are associated with increased SO_2 emissions during combustion or H_2S and COS during gasification. Similarly, Karvina2 showed lower nitrogen content in the combustible fraction (N_{ad} = 0.73 wt.%) than the other samples (N_{ad} = 1.01–1.04 wt.%). Chlorine content was also lowest in Karvina2 (Cl^a = 0.036 wt.% in coal and 0.009 wt.% in mineral fraction) compared to the other samples

(Cl[a] = 0.054 wt.% in coal and 0.018 wt.% in mineral fraction). Elevated chlorine levels can exacerbate slagging, deposit formation, agglomeration, and corrosion of combustion components. However, the chlorine levels across all samples remained within the typical range for energy coals.

2.5. Ash composition and characteristic ash fusion temperatures analyses

The characteristic ash fusion temperatures of the tested samples, both coal and mineral fractions (Table 33), exceed 1200°C, which indicates that there should be no issues related to agglomeration and slagging during the calcination of these fractions in a fluidized bed reactor. However, the implementation of the concept of using the fraction enriched with combustible compounds after separation in dust furnaces should be approached with caution. The deformation temperature (DT) and sphere temperature (ST) in a reducing atmosphere fall within the ranges of 1220–1290°C and 1380–1450°C, respectively. In the flame core, under air staging conditions—which is a common practice—such high temperatures and reducing conditions may occur.

Table 33 Characteristic ash melting temperatures of coal and mineral fraction.

Parameter		Unit	Haldex 1		Haldex 2		Karvina 2	
			Coal fraction	Mineral fraction	Coal fraction	Mineral fraction	Coal fraction	Mineral fraction
Oxidising atmosphere	Deformation temperature, DT	°C	1360	1350	1390	1350	1330	1430
	Sphere temperature, ST	°C	1450	1480	1510	1460	1420	1530
	Hemisphere temperature, HT	°C	1481	1520	1520	1490	1440	1560
	Flowing temperature, FT	°C	1500	1540	1540	1510	1460	1580
Reducing atmosphere	Deformation temperature, DT	°C	1220	1330	1290	1330	1210	1420
	Sphere temperature, ST	°C	1380	1420	1450	1390	1350	1490
	Hemisphere temperature, HT	°C	1430	1450	1470	1420	1390	1520
	Flowing temperature, FT	°C	1450	1490	1490	1460	1410	1550

The results of the analyses of the chemical composition of ash for the coal and mineral fractions are presented in Table 34 and Table 35.

.

Table 34 Chemical composition of ash coal fraction.

Type of research/ Research method		Symbol	Unit	Carbon-bearing jig product Haldex 1	Carbon-bearing jig product Haldex 2	Carbon-bearing jig product Karvina 2	HALDEX-material for gasification
Chemical composition of ash in terms of oxides Q/LCA/55/B:2022 (met. ICP-OES)	Silicon dioxide	SiO2	%	47.72	47.83	51.92	45.22
	Aluminium oxide	Al2O3	%	27.92	28.79	25.97	29.96
	Diferrous trioxide	Fe2O3	%	5.35	5.64	5.41	5.71
	Calcium oxide	CaO	%	3.47	2.51	4.28	3.51
	Magnesium oxide	MgO	%	2.47	2.09	2.44	2.30
	Disodium oxide	Na2O	%	0.54	0.50	0.45	0.76
	Dipotassium oxide	K2O	%	2.56	2.61	3.08	2.54
	Titanium dioxide	TiO2	%	1.05	1.12	1.12	1.22
	Trimanganese tetroxide	Mn3O4	%	0.07	0.06	0.11	0.07
	Diphosphorus pentoxide	P2O5	%	1.03	0.86	0.28	1.27
	Sulfur trioxide	SO3	%	2.65	1.91	1.70	2.87
	Barium oxide	BaO	%	0.15	0.15	0.07	0.20
	Strontium oxide	SrO	%	0.12	0.12	0.04	0.18
Elemental content in fuel on dry basis (from calculations) Q/LCA/55/B:2022 (met.ICP-OES)	Silicon	Sid	%	5.090	4.885	9.812	3.437
	Aluminum	Ald	%	3.372	3.329	5.557	2.578
	Sodium	Nad	%	0.091	0.081	0.136	0.091
	Potassium	Kd	%	0.485	0.474	1.033	0.342
	Magnesium	Mgd	%	0.340	0.275	0.595	0.226
	Titanium	Tid	%	0.144	0.146	0.271	0.119
	Strontium	Srd	%	0.023	0.022	0.015	0.024

Table 35 Chemical composition of ash mineral fraction.

Type of research/Research method		Symbol	Unit	Haldex1	Haldex2	Karvina2	HALDEX material for calcination
Chemical composition of ash in terms of oxides Q/LCA/55/B:2022 (met. ICP-OES)	Silicon dioxide	SiO2	%	57.09	58.69	56.97	64.50
	Aluminium oxide	Al2O3	%	23.03	22.12	25.20	23.15
	Diferrous trioxide	Fe2O3	%	5.87	5.93	4.59	4.13
	Calcium oxide	CaO	%	0.47	0.77	0.70	0.20
	Magnesium oxide	MgO	%	1.72	1.83	1.62	1.57
	Disodium oxide	Na2O	%	0.33	0.31	0.31	0.45
	Dipotassium oxide	K2O	%	3.31	3.20	3.74	3.58
	Titanium dioxide	TiO2	%	0.95	0.93	1.00	1.01
	Trimanganese tetroxide	Mn3O4	%	0.06	0.07	0.06	0.05
	Diphosphorus pentoxide	P2O5	%	0.13	0.23	0.13	0.09
	Sulfur trioxide	SO3	%	0.38	0.60	0.25	0.15
	Barium oxide	BaO	%	0.06	0.06	0.06	0.06
	Strontium oxide	SrO	%	0.01	0.02	0.02	0.02
Elemental content in fuel on dry basis (from calculations) Q/LCA/55/B:2022 (met. ICP-OES) Q/LCA/55/B:2022 (met. ICP-OES)	Silicon	Sid	%	22.480	22.706	22.438	26.772
	Aluminum	Ald	%	10.269	9.692	11.238	10.878
	Sodium	Nad	%	0.204	0.188	0.195	0.297
	Potassium	Kd	%	2.317	2.198	2.618	2.640
	Magnesium	Mgd	%	0.876	0.913	0.823	0.841
	Titanium	Tid	%	0.481	0.460	0.504	0.538
	Strontium	Srd	%	0.010	0.012	0.013	0.012

Results of analysis indicated that all samples are silicon-aluminium rich materials, which can be used for geopolymer membranes preparation. In the mineral fraction, the most important parameter, from the perspective of the specific goal (i.e., geopolymer production), is the $SiO_2/Al2O_3$ ratio. The obtained values, ranging from 3.8 to 4.5, are typical of those used by other researchers and are nearly in the middle of the applied scale (i.e., 2.0–7.0).

2.6. Trace element analysis

Table 36 and Table 37 present the trace element contents of the coal and mineral fractions after the separation of post-mining waste.

Table 36 Analysis of trace elements in coal fraction.

Type of research/Research method		Symbol	Unit	Carbon-bearing jig product Haldex 1	Carbon-bearing jig product Haldex 2	Carbon-bearing jig product Karvina2	HALDEX2 - material for gasification
Content of trace elements (dry basis) Q/LCA/57/B:2022	Beryllium	Be	mg/kg	2.79	2.77	2.91	2.41
	Cobalt	Co	mg/kg	8.49	9.35	9.17	7.87
	Europium	Eu	mg/kg	0.603	0.528	0.748	0.356
	Gallium	G	mg/kg	8.17	8.29	13.7	7.10
	Antimony	Sb	mg/kg	2.60	2.40	2.15	2.43
	Molybdenum	Mo	mg/kg	1.84	1.80	0.894	2.14
	Nickel	Ni	mg/kg	28.7	27.7	30.4	26.3
	Scandium	Sc	mg/kg	4.35	3.03	6.51	3.56
	Samarium	Sm	mg/kg	2.79	1.92	2.85	1.62
	Tungsten	W	mg/kg	1.40	1.37	0.819	1.09
	Yttrium	Y	mg/kg	7.38	1.87	20.6	6.42
	Ytterbium	Yb	mg/kg	1.16	0.971	1.25	0.710
	Lithium	Li	mg/kg	49.8	52.6	78.1	64.6

Table 37 Analysis of trace elements in mineral fraction.

Type of research/Research method		Symbol	Unit	Haldex1	Haldex2	Karvina2	HALDEX material for calcination
Content of trace elements (dry basis) Q/LCA/57/B:2022	Beryllium	Be	mg/kg	2.64	2.64	2.95	2.70
	Cobalt	Co	mg/kg	17.6	17.4	18.3	22.7
	Europium	Eu	mg/kg	0.425	0.435	0.333	0.305
	Gallium	Ga	mg/kg	25.1	23.2	26.0	25.2
	Antimony	Sb	mg/kg	3.87	3.93	4.11	3.24
	Molybdenum	Mo	mg/kg	0.674	0.668	0.460	0.650
	Nickel	Ni	mg/kg	44.9	43.6	43.1	49.0
	Scandium	Sc	mg/kg	21.2	21.7	19.4	24.4
	Samarium	Sm	mg/kg	15.1	14.7	16.6	20.0
	Tungsten	W	mg/kg	3.35	2.24	3.04	3.50
	Yttrium	Y	mg/kg	4.21	4.31	4.42	4.28
	Ytterbium	Yb	mg/kg	0.722	0.776	6.65	0.617
	Lithium	Li	mg/kg	105	106	125	150

In each of the analysed samples, the elements with the highest share (both in the raw state and in the coal and mineral fractions after separation) were: lithium (49.8-140 mg/kg), nickel (27.7-46.4 mg/kg), scandium (3.0-23.9 mg/kg), cobalt (8.5-19.8 mg/kg) and gallium (21.1-23.3 mg/kg). The content of the remaining trace elements was at the level of <10 mg/kg, and their content was similar to those in samples analysed by other researchers. It is also worth emphasizing that in the mineral fraction the content of individual trace elements is much higher than in the carbon fraction - the exception to this rule is the content of europium and molybdenum, but the differences between both fractions are very small.

2.7. Heavy metals analysis

Table 38 presents the contents of heavy metals present in the coal fraction without division into fractions.

Table 38 Analysis of heavy metals content in Haldex1, Haldex2 and Karvina2 coal fraction samples.

Type of test / Research method		Symbol	Unit	Carbon-bearing jig product HALDEX1	Carbon-bearing jig product HALDEX2	Carbon-bearing jig product KARVINA2
Content of heavy metals elements (dry basis) Q/LCA/57/B:2022	Arsenic	As	mg/kg	2.50	2.51	5.27
	Cadmium	Cd	mg/kg	0.739	0.771	0.984
	Chromium	Cr	mg/kg	39.3	40.5	56.6
	Copper	Cu	mg/kg	53.7	48.6	35.2
	Nickel	Ni	mg/kg	20.9	21.1	22.2
	Lead	Pb	mg/kg	23.6	18.2	22.4
	Zinc	Zn	mg/kg	54.9	51.9	63.6
Content of heavy metals elements (dry basis) Q/LCA/32/B:2022	Mercury	Hg	mg/kg	0.046	0.06	0.046

Additionally, the coal fraction was divided into three grain fractions, i.e. >10 mm; 10-3.15 mm and <3.15 mm. For each fraction (after separation), the content of heavy metals was analyzed. Table 39 shows the results of the trace element analysis depending on the fraction for the Haldex 1 sample, while Table 39– for the Karvina 2 sample.

Table 39 Heavy metals analysis results for the Haldex 1 sample by fractions.

Type of test / Research method		Symbol	Unit	Raw (basic)	>10 mm	10.0-3.15 mm	<3.15 mm
Content of heavy metals (dry basis) Q/LCA/57/B:2022	Arsenic	As	mg/kg	2.50	2.20	3.47	3.82
	Cadmium	Cd	mg/kg	0.739	1.10	1.12	1.22
	Chromium	Cr	mg/kg	39.3	38.1	43.7	81.8
	Copper	Cu	mg/kg	53.7	55.5	51.2	41.9
	Nickel	Ni	mg/kg	20.9	23.5	25.0	34.5
	Lead	Pb	mg/kg	23.6	23.8	30.1	28.5
	Zinc	Zn	mg/kg	54.9	32.0	60.2	122.9
Content of heavy metals (dry basis) Q/LCA/32/B:2022	Mercury	Hg	mg/kg	0.046	0.069	0.181	0.104

Table 40 Heavy metals analysis results for the Karvina 2 sample by fractions.

Type of test / Research method		Symbol	Unit	Raw (basic)	>10 mm	10.0-3.15 mm	<3.15 mm
Content of heavy metals (dry basis) Q/LCA/57/B:2022	Arsenic	As	mg/kg	5.27	8.48	5.85	7.00
	Cadmium	Cd	mg/kg	0.984	1.22	1.30	1.31
	Chromium	Cr	mg/kg	56.6	46.6	56.4	74.3
	Copper	Cu	mg/kg	35.2	36.2	35.9	45.4
	Nickel	Ni	mg/kg	22.2	22.4	21.1	31.7
	Lead	Pb	mg/kg	22.4	29.8	29.7	31.5
	Zinc	Zn	mg/kg	63.6	38.9	53.8	194.4
Content of heavy metals (dry basis) Q/LCA/32/B:2022	Mercury	Hg	mg/kg	0.046	0.141	0.166	0.159

Figure 9 presents the total content of heavy metals (excluding mercury) in samples depending on the particle size of the sample.

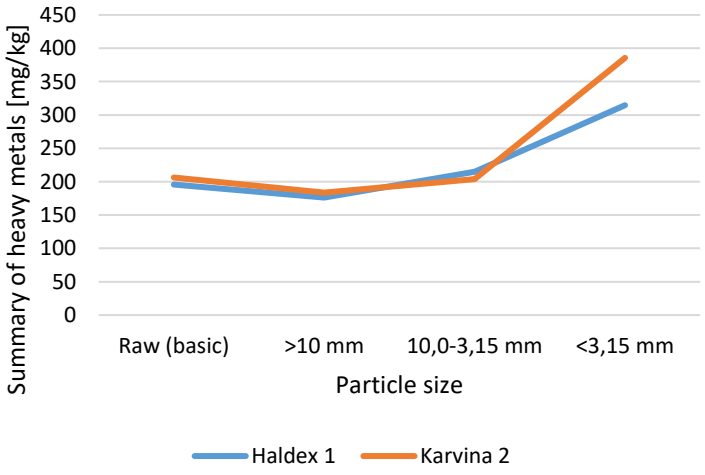

Figure 9 Total content of heavy metals (excluding mercury) in Haldex 1 and Karvina 2 samples depending on the particle size of the sample.

Based on the results, it can be seen that generally the finer coal fraction, the higher content of individual heavy elements. The fraction with grain size <3.15 mm contains the highest content of heavy metals. The total content of heavy metals in both analysed samples (after separation to individual fractions) was similar, and for grain size <3.15 mm it was 315 mg/kg (Haldex1 sample) and 385 mg/kg (Karvina2 sample). In the base samples (before separation) the total content of heavy metals was 195 and 206 mg/kg, respectively.

The mercury content depending on the particle size in the analysed samples is presented in Figure 10.

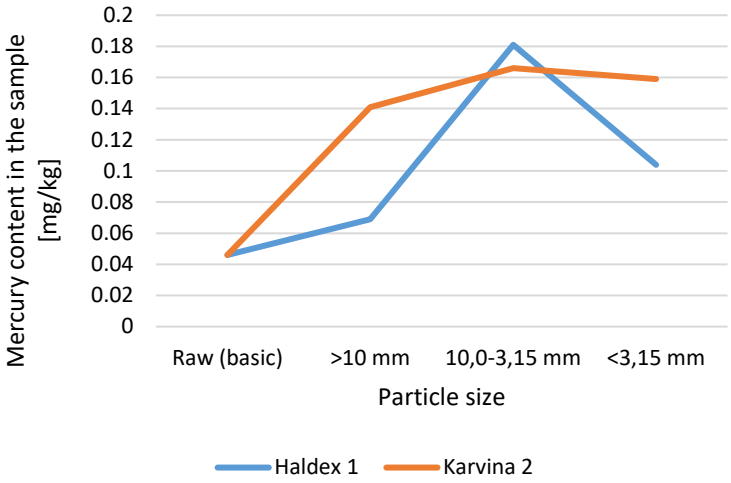

Figure 10 Mercury content in coal fractions in Haldex 1 and Karvina 2 depending on particle size of the sample.

As with other heavy metals, finer coal fractions tend to accumulate more mercury. In the case of the highest mercury, the largest amount of it was accumulated in the fraction with grain size of 10.0-3.15 mm, for both Haldex1 and Karvina2 samples.

2.8. Microscopic morphological examination

Microscopic analysis was conducted to identify textural and structural features indicative of thermal or chemical alteration of organic matter in mine heap samples. Enriched waste samples were examined using an AxioImager M1m polarizing microscope (as in T2.2), focusing on material composition and potential changes in organic matter due to temperature effects, oxidation, weathering, or degassing. Reflectance analysis (PN-ISO 7404-5:2002) was also performed to determine the degree of coalification and sample homogeneity.

Table 41 demonstrates that all three samples were significantly enriched in organic matter. However, a side effect of the enrichment process was a noticeable reduction in the grain size of coal particles. Despite this, the samples displayed a high degree of homogeneity. Test results confirmed earlier findings (from fresh coal fractions in mining

heaps) that the samples likely originated from the same mine or from multiple mines with identical petrographic coal deposit characteristics. Samples Haldex1 (coal fraction) and Haldex 2 (coal fraction) exhibited broader reflectogram bases, resembling those obtained during the analysis of fresh mine wastes prior to enrichment.

Table 41 Mean random vitrinite reflectance values of the carbon-bearing jig samples.

Sample	VR_0 [%]	Reflectance histogram
HALDEX 1	0.83	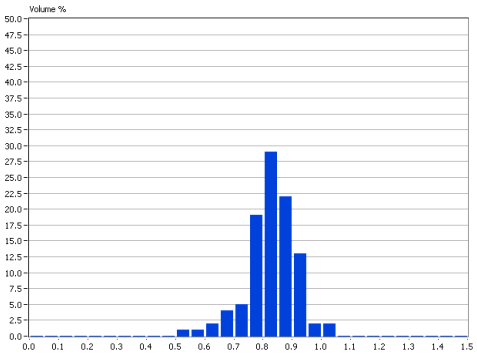
HALDEX 2	0.85	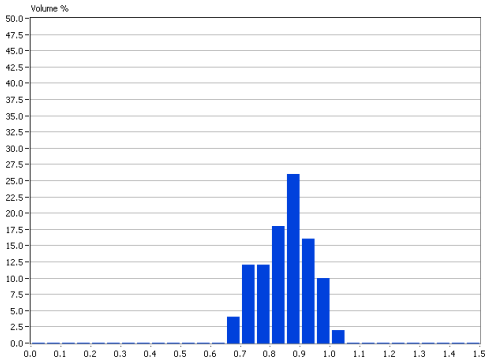
KARVINA 2	0.88	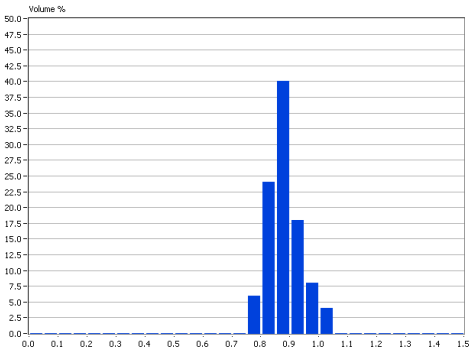

Microscopic morphological analysis of the enriched samples revealed no visible signs of thermal or chemical transformations of the organic matter (Figure 11). Observing surface changes was more challenging due to sample grinding during the enrichment process, making it difficult to determine which grain surfaces were exposed to oxidation in the dumps. No evidence of oxidation, gasification, or pyrolysis processes was detected. While partial weathering of organic matter cannot be ruled out, its symptoms would require detailed geological analysis of the raw material in the source deposit for confirmation. The microscopic examination yielded similar conclusions regarding coalification levels, vitrinite class distribution, and alteration indicators as the analysis of fresh, unenriched wastes.

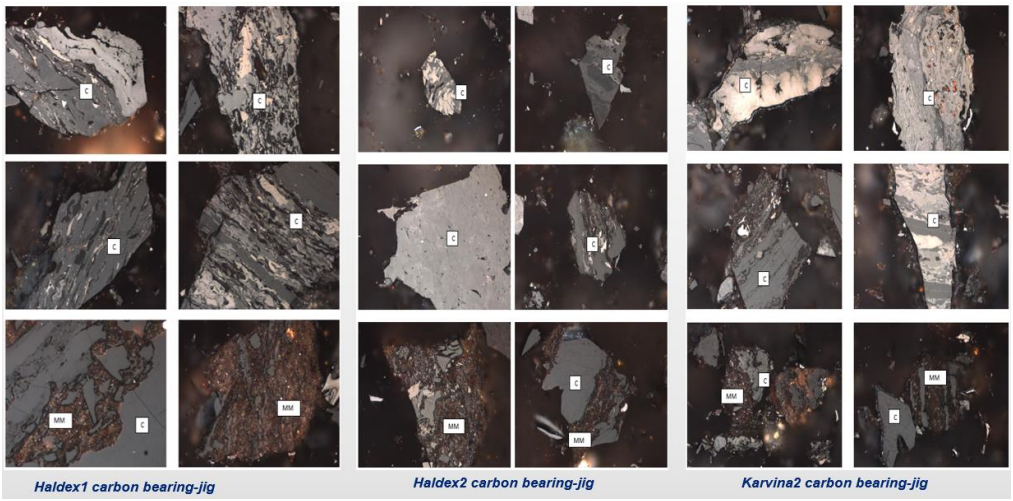

Figure 11 Exemplary photomicrographs of carbon bearing jig product (white light, reflected, oil immersion, area ×500) C- coal; MM – mineral matter.

The primary and expected distinction between raw and enriched waste samples was the significant reduction in mineral matter content. The remaining mineral matter primarily consisted of fine clay minerals embedded as overgrowths within the coal. Additionally, the grain size of both organic and inorganic components in the enriched samples was markedly finer compared to the raw material.

2.9. The results of the XRF analysis

For the fractions obtained from raw mining waste, including both the mineral and coal fractions, a detailed oxide composition analysis was conducted using XRF analysis. This analysis enabled the identification of present mineral phases and the quantitative determination of individual oxides in the tested samples. The obtained results provided essential information on the characteristics of the waste, which is crucial for further processing and potential applications in various industries. The results are presented in Table 42 and Table 43.

Table 42 Oxide composition of mineral fraction from the XRF analysis.

	Haldex 1	Haldex2	Karvina2
	mineral fraction	mineral fraction	mineral fraction
SiO2	50.6	51.8	48.9
Al2O3	22.4	23.5	23.5
Fe2O4	4.41	3.66	3.68
CaO	0.45	0.31	0.50
MgO	1.52	1.45	1.30
TiO2	0.95	0.98	0.93
MnO	0.04	0.03	0.05
K2O	2.93	3.04	3.30
Na2O	0.3	0.3	0.3
P2O5	0.13	0.10	0.11
Loss by ignition	16.2	14.7	17.4

Table 43 Oxide composition of coal-bearing fraction from the XRF analysis.

	Haldex 1	Haldex2	Karvina2
	Coal-bearing fraction	Coal-bearing fraction	Coal-bearing fraction
SiO2	25.7	25.2	28.3
Al2O3	14.0	14.0	15.1
Fe2O4	2.34	1.94	3.20
CaO	0.86	0.81	2.18
MgO	1.03	0.89	1.38
TiO2	0.56	0.56	0.59
MnO	0.02	0.02	0.06
K2O	1.73	1.85	1.93
Na2O	0.3	0.3	0.2
P2O5	0.20	0.31	0.13
Loss by ignition	52.9	53.8	46.3

Table 44 SO_3 content in mineral and coal-bearing fractions.

Sample	SO_3 content
Haldex 1 Coal-bearing	0.41
Haldex 1 Mineral	0.06
Haldx 2 Coal-bearing	0.28
Haldex 2 Mineral	< 0.05
Karviná 2 Coal-bearing	0.58
Karviná 2 Mineral	< 0.05

2.9.1. The results of the XRD analysis

The samples of the separation from the same source have the same mineral but differ by quantity. Individual samples are similar but in different quantities, as demonstrated by XRF analysis. In all samples, the main minerals were quartz, kaolinite, halloysite, illite, muscovite, and sometimes dolomite. The same results were obtained by analyzing the raw mine samples. The main difference consists of combustible matter content, as illustrated by mass loss by ignition.

The SO_3 content in samples is related to coal-bearing. Indeed, as Table 44 shows, the SO_3 content and the mass loss by ignition are too high.

Regarding the combustible matter content in the coal-bearing sample, we analysed only the mineral-bearing samples using a thermal method. The first essay on thermal measurement of the coal-bearing sample damaged the apparatus and evolved a harmful gas.

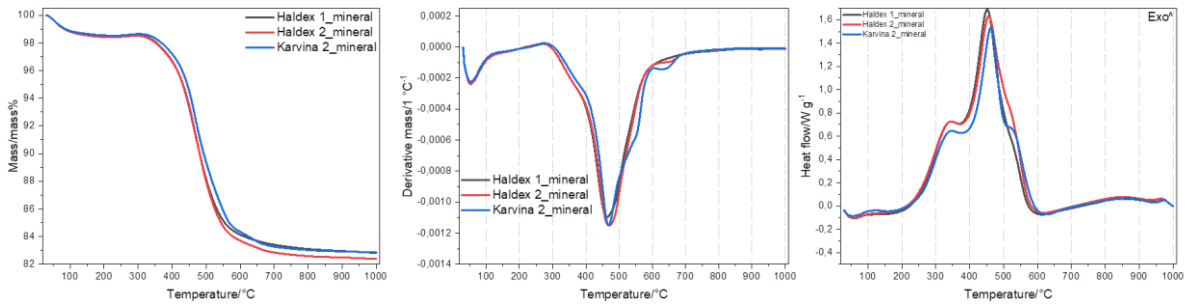

A B C

Figure 12 TG, DTG and DSC curves of mineral-bearing samples.

Observing the three types of curves (TG, DTG, DSC of the mineral-bearing and coal-bearing samples) gives insight into the thermal behaviors of exothermic and endothermic processes occurring during the thermal treatment of raw materials. Indeed, the DSC curves signal the exothermic reactions of the oxidation of organic matter contained in raw mine samples. It is clear that the mineral-bearing samples still contain volatile matter (SO_3, organic matter, and water chemically bound in kaolinite). The DTG curves describe the process rate related to the mass loss during the thermal treatment. The mass loss for all mineral-bearing samples corresponds to the results of loss by ignition reported in Table 42 and Table 43. The mass loss is due to the evolved volatile organic matter, sulfur oxidation, and clay dehydroxylation. The dehydroxylation of kaolinite occurs at this temperature range, with the onset of the transformation to metakaolin. The process can be mostly described by the reaction:

$$2Al_2Si_2O_5OH = 2Al_2Si_2O_7 + 4H2O$$

The TG curves report the total amount of matter removed from the samples after thermal processing to 1000 °C.

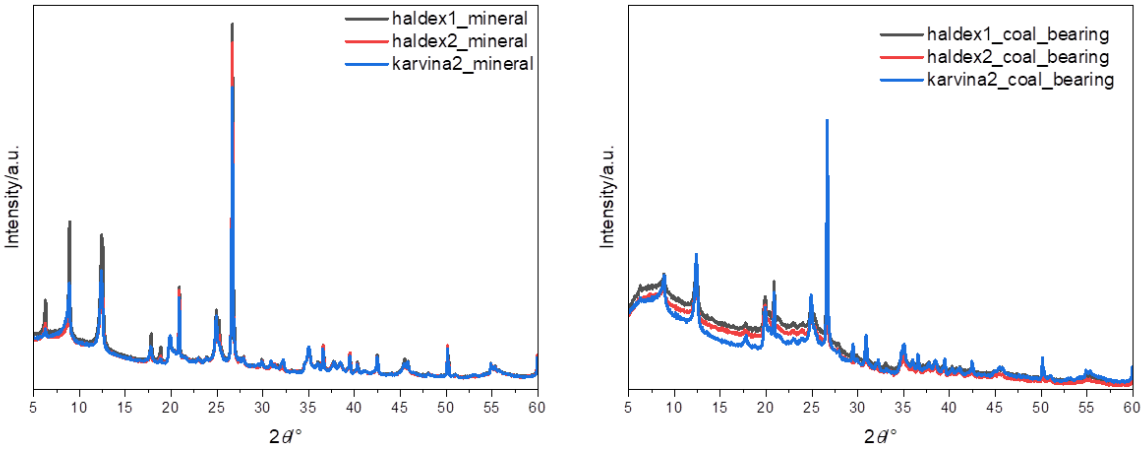

A B

Figure 13 XRD of mineral-bearing samples (A) and coal-bearing samples (B).

The minerals in mineral-bearing and coal-bearing samples are qualitatively similar but differ by quantity, as illustrated by the peak intensities. XRD of coal-bearing samples presents some amorphous characteristics due to the presence of no-well crystallized organic compounds. The intensities of the peaks are reduced by

comparison with XRD mineral-bearing samples. By observing the different peak positions, it is clear that the phases are similar in all three types of samples from both categories. Quartz and kaolinite are the dominant phases. The endothermic peak located at 400-600°C on the DTG curves illustrates kaolinite's presence.

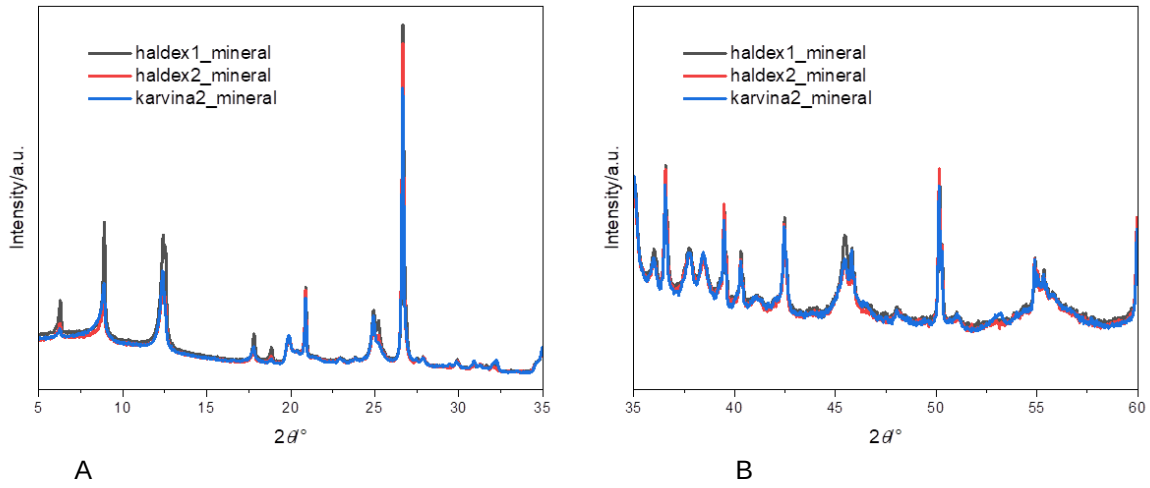

Figure 14 XRD of mineral-bearing samples (A: 5-30) and (B: 30-50).

The minerals in mineral-bearing samples are qualitatively similar but differ by quantity, as illustrated by the peak intensities.

Figure 15 shows an enlarged view of Figure 14 A to illustrate the similarities or identify the differences between the peaks of mineral-bearing samples. As can be seen, the differences in intensity are minimal, but the similarities between the peaks are obvious. The results of XRF confirm that the oxide composition is too similar (Table 42).

The main phases identified by XRD in different samples are summarized as follows:

Haldex 1_coal bearing: quartz (SiO_2), kaolinite [$Al_2Si_2O_5(OH)_4$]; halloysite10Å($Al_2Si_2O_5(OH)_4.nH_2O$); $CaAl_2((OH)_8(H_2O)_2)(H_2O)_{1,84}$;

Haldex 1_mineral: quartz (SiO_2), kaolinite [$Al_2Si_2O_5(OH)_4$]; halloysite10Å ($Al_2Si_2O_5(OH)_4.nH_2O$);

Haldex 2_ coal bearing: quartz (SiO_2), kaolinite [$Al_2Si_2O_5(OH)_4$]; dolomite [$CaMg(CO_3)_2$]; muscovite $2M_1$ $KAl_2(Si_3Al)O_{10}(OH)_2$.

Haldex 2_mineral: quartz (SiO_2), kaolinite [$Al_2Si_2O_5(OH)_4$]; sľuda polytyp;

Karviná 2_coal bearing: quartz (SiO_2), kaolinite1A $[Al_2Si_2O_5(OH)_4]$; illite 2M1$(K1–1.5A_{14}[Si_{7–6.5}A_{11–1.5}O_{20}](OH_4)$; dolomite $[CaMg(CO_3)_2]$;

Karviná 2_mineral: quartz (SiO_2); kaolinite1*A* $[Al_2Si_2O_5(OH)_4]$; muscovite $KAl_2(Si_3Al)O_{10}(OH)_2$; $CaAl_2O_4 \cdot 10H_2O$.

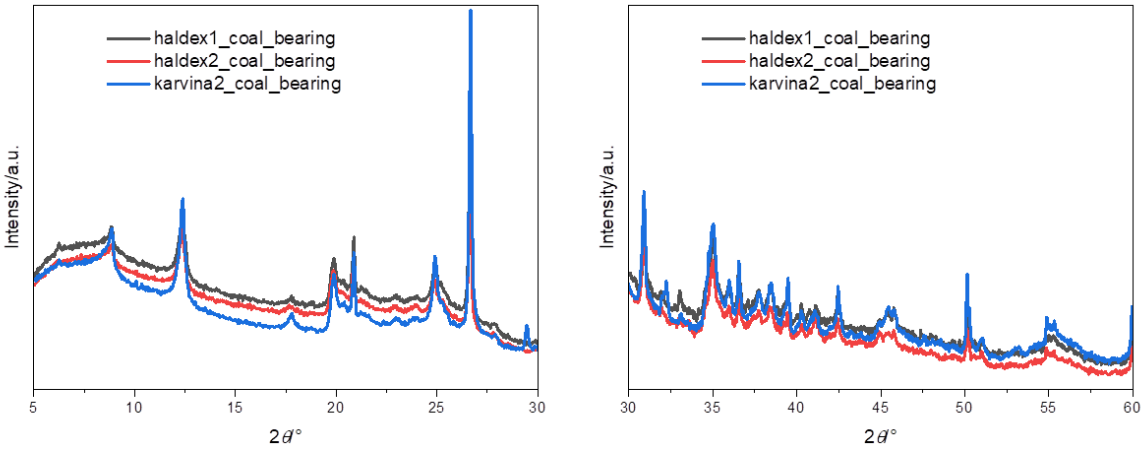

A B

Figure 15 XRD details of coal-bearing samples (A: 5-30) and (B: 30-50).

The minerals in coal-bearing samples are qualitatively similar but differ by quantity, as illustrated by the peak intensities.

Figure 15. represents a detailed view of Figure 14 B, in which one can see that the background of peaks in some areas illustrates the presence of no-well crystallized matter. This is related to the presence of volatile matter, namely coal-containing. The mass loss by ignition of coal-bearing samples is Haldex1-coal bearing (52.9%), Haldex2-coal bearing (53.8%), and Kraviná 2-coal bearing (46.3%).

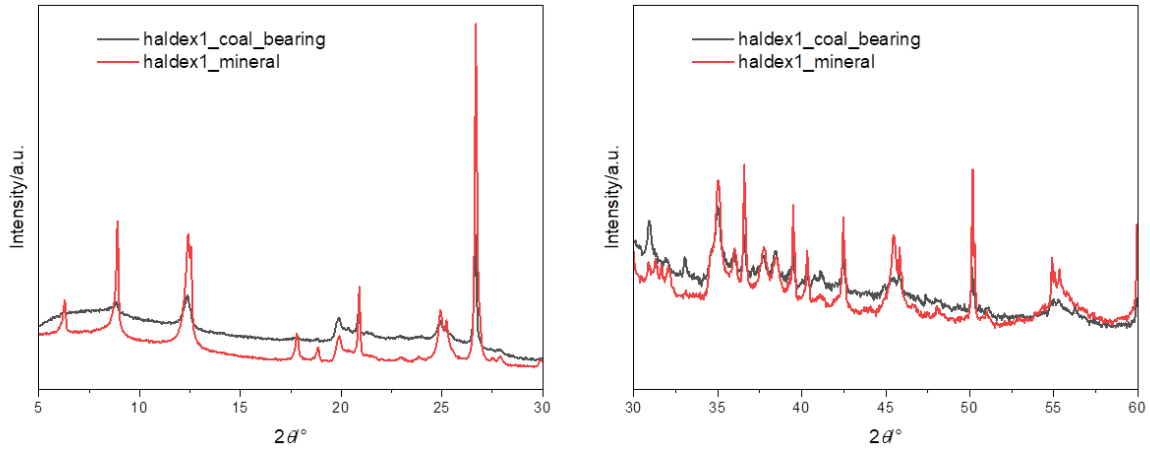

Figure 16 XRD comparison between Haldex 1 mineral bearing and coal-bearing sample (A: 5-30) and (B: 30-50).

It is evident that the peaks shown in Figure 16 (Haldex1) for the mineral-bearing samples are more pronounced and higher than those for the coal-bearing samples. The pseudo-new peaks appearing at 2θ=6, 17,8, and 18 in Figure 16. of mineral-bearing samples are not entirely new; they are also in coal-bearing samples but masked due to the higher organic matter content.

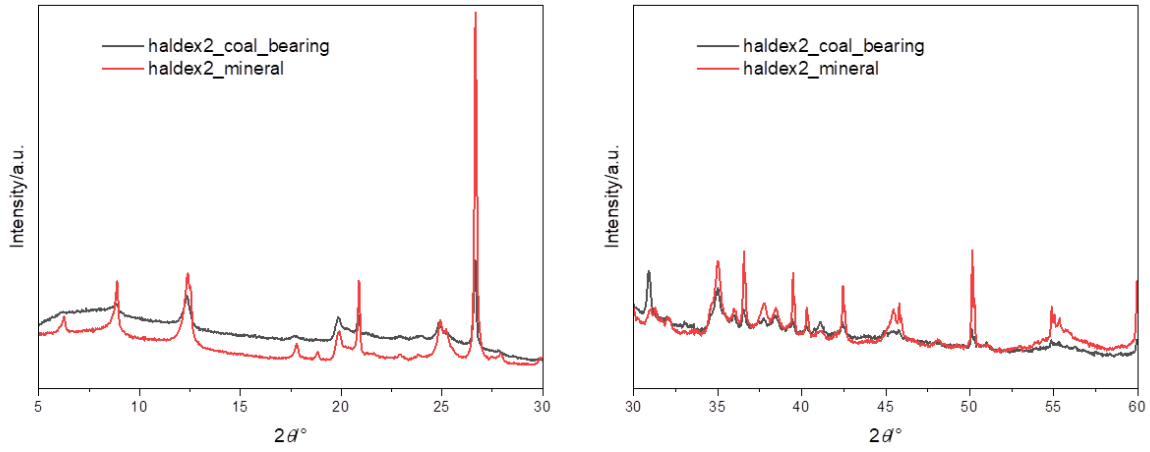

Figure 17 XRD comparison between Haldex 2 mineral sample and coal-bearing sample (A: 5-30) and (B: 30-50).

Figure 17 (Haldex 2) for the mineral-bearing samples shows a more pronounced and higher peaks than those for the coal-bearing samples. The new peaks appearing

at 2θ= 6, 17,8, and 18 in Figure 17 of mineral-bearing samples confirm that the separation technology has led the change in mineralogical composition and that the coal bearing part will be suitable for the hydrogen production.

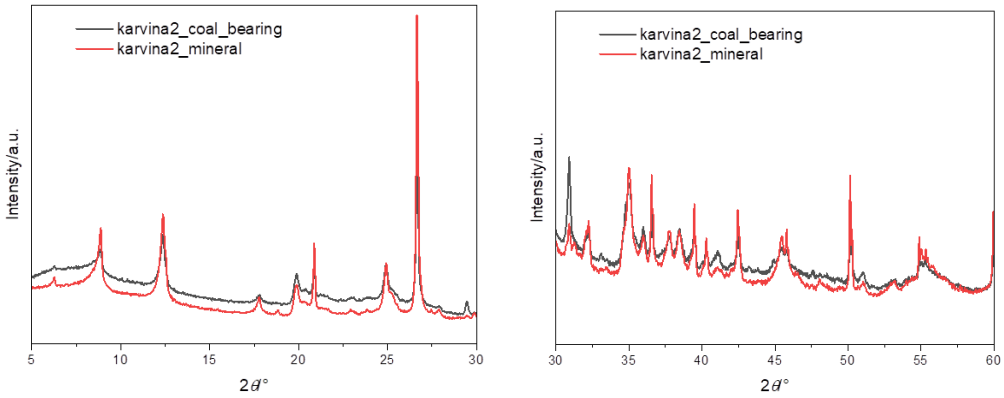

Figure 18 XRD comparison between Karviná 2 mineral sample and coal-bearing sample (A: 5-30) and (B: 30-50).

The XRD depicted in Figure 18 (Kravina 2) for the mineral-bearing samples is more pronounced and higher than those for the coal-bearing samples. Qualitatively, the mineral composition is the same, but quantitatively, it differs due to the organic matter content. Considering the loss by ignition and the content of SO_3 in Table 45, it is evident that the coal-bearing sample has a higher content of volatile matter. The presence of sulfur is illustrated by the exothermic peak at the DSC curves (Figure 12) at temperatures between 200°C and 350°C. Considering the high content of volatile matters (organic, sulfuric) determined by the ignition method, we have not done the thermal analysis of coal-bearing samples for the safety reasons of the apparatus.

Table 45 Considering the loss by ignition and the content of SO_3.

Sample	Loss by ignition	SO_3
Haldex 1 mineral fraction	16.2	0.06
Haldex 1 coal-bearing	52.9	0.41
Haldex2 mineral fraction	14.7	< 0.05
Haldex 2 coal-bearing	53.8	0.28
Karvina 2 mineral fraction	17.4	< 0.05
Karvina 2 coal-bearing	46.3	0.58

3. Conclusions

1. The analysis of the samples from the laboratory process of jig beneficiation, obtained from the separation of mining waste collected from dumps located in Poland and the Czech Republic, revealed significant variability in terms of the examined quality parameters. This variability included both the grain size composition and density composition of the delivered samples, as well as sulphur content, ash content, and the associated calorific value (Figure 19).

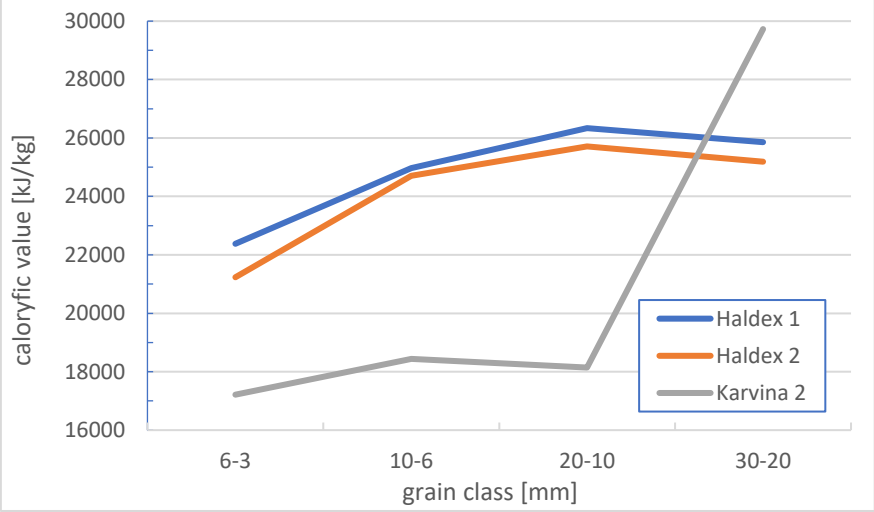

Figure 19 Calorific value in different grain classes for three types of the carbon-bearing product.

2. The grain size analysis showed a significantly higher share of fine grains in product samples from the separation of Haldex and Karvina materials, especially in the combustible products. The shares of grain classes in all analyzed products are shown in Figure 20.

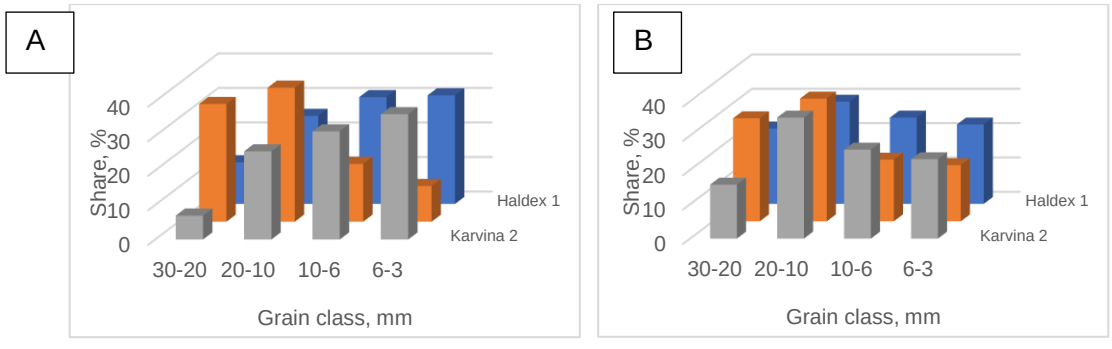

Figure 20 Grain class shares in of the carbon-bearing product (A) and mineral (B) products.

3. A parameter that differed significantly in the various samples was the share of combustible fractions, i.e., the sum of the coal grains <1.5 g/cm³ and intermediate fractions (1.5-1.8 g/cm³), in combustible product. Larger shares of the above-mentioned fractions in the carbon-bearing product were observed in each case in coarser grains – the 30-10 mm class. The obtained values ranged from 84.84% (Karvina 2) to 94.82% (Haldex 2), with the majority consisting of grains with a density of <1.5 g/cm³. The shares of the entire analysed material (30-3 mm class) in the carbon-bearing product ranged from 70.20% (Karvina 2) to 91.36% (Haldex 2). In each of the samples, the mineral product in the 30-3 mm size class was characterized by a very low content of combustible fractions, ranging from 2.07% to 3.56%.

4. Based on the density-quality analysis, the carbon-bearing product Haldex 1 and Haldex 2 exhibited significantly higher average calorific values (24.503 kJ/kg and 25.194 kJ/kg, respectively) compared to the Karvina 2 sample (19.036 kJ/kg). The lowest average calorific values were found in the mineral products Karvina 2 (1.813 kJ/kg) and Haldex 1 (1.907 kJ/kg). The calorific values of the analysed products are shown in Figure 21.

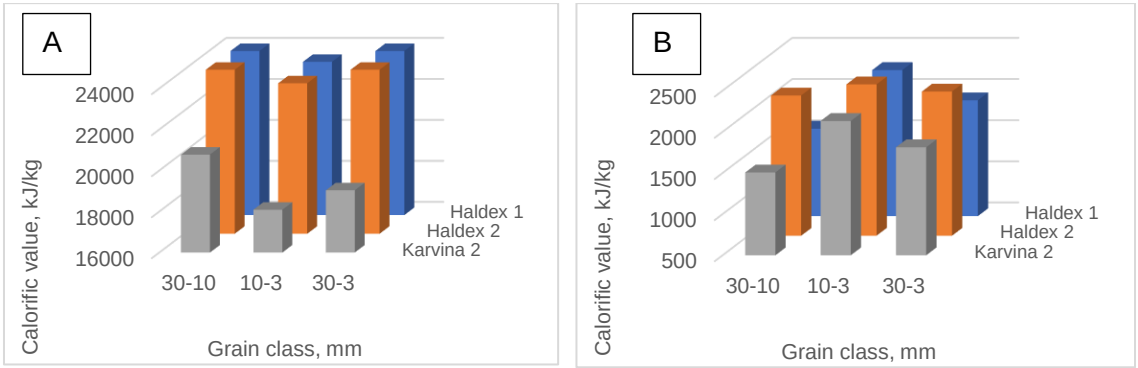

Figure 21 Calorific value in the carbon-bearing product (A) and mineral (B) products.

5. All mineral products were characterized by high ash content, exceeding 82% in each case. The lowest ash content was found in the carbon-bearing product samples Haldex 1 (21.83%) and Haldex 2 (19.06%).

6. The analysed samples also differed in sulphur content. The highest sulphur values in the carbon-bearing product were found in the Haldex 1 (0.75%) and Haldex 2 (0.84%) samples, while in the mineral products, the highest sulphur content was in the Haldex 1 (0.62%) and Haldex 2 (0.54%) samples. The lowest sulphur content was found in the Karvina 2 sample 0.43% for the carbon-bearing product and 0.09% for the mineral product.
7. The analysis of the quality parameters of the samples indicates that the application of the beneficiation process in a pulsating water medium may enable the production of the carbon-bearing product with significant calorific value, which allows for its further use in hydrogen production. Additionally, the mineral product with minimized content of combustible fraction grains can be used for further processing to produce new valuable materials, including geopolymers.
8. **Determination of the crushing resistance of aggregates:** Samples H1/2 and H2/2, which have results above 30, might require the use of aggregates with better abrasion resistance to meet the PN-EN 1097-2 standard. K2/2 and H/GIG seem acceptable for construction use, but further verification of their mechanical properties may be needed depending on the project requirements.
9. **Determination of the abrasion resistance of aggregates -** all samples (Haldex 1, Haldex GIG, Haldex 2, Karvina 2) have Micro-Deval results that exceed 20%, indicating very poor resistance to abrasion compared to the requirements of PN-EN 1097-1 for aggregates used in road or concrete construction. Therefore: None of these materials meet the requirements of PN-EN 1097-1 for aggregates used in road surfaces or concrete because their abrasion resistance is far too low. It is recommended to look for other materials that meet the PN-EN 1097-1 standards (with results below 20% for Micro-Deval), especially for applications requiring high durability and resistance to wear.
10. **Water absorbtion** - The analysis of water absorption for samples in different grain size classes (4-8 mm, 8-16 mm, 16-32 mm) shows varying levels of water absorption, indicating differences in porosity and material structure:

- Class 4-8 mm: The H1/m/4-8 sample has the highest water absorption (9%), and H2/m/4-8mm has slightly lower absorption (8%). H/m/4-8 has the lowest absorption (5-6%), and K2/m/4-8mm falls in the medium range (7%). According to the European standard, water absorption should not exceed 1% to guarantee frost resistance, so none of the samples in this class meet this requirement.
- Class 8-16 mm: Similar to the 4-8 mm class, the H1/m/4-8 sample has the highest water absorption (9%), and the K2/m/4-8 sample falls in the medium range (7%).
- Class 16-32 mm: The H1/m/s16-32 sample has the highest water absorption (4%), and H2/m/s16-32mm (3.7%) shows slightly lower absorption. The other samples in this class have progressively lower water absorption, indicating moderate water absorption.

All samples have higher water absorption than the required 1%, meaning they do not meet the European standard for frost resistance.

11. **Frost resistance** - depending on the frost resistance requirements of the project, K2/m/8-16mm and H2/m/16-32mm show the best performance, while H1/m/8-16mm and H1/m/16-32mm should be avoided in more demanding conditions.
12. **SEM EDS** - The analyses showed that in the H1/m, H2/m, H/m, and K2/m samples, Si is the dominant component, with an average content ranging from 15.95 to 21.64 % by weight, followed by Fe with an average from 10.50 to 13.49 % by weight, and Al with an average from 8.11 to 10.42 % by weight. In the H1/m sample, Ba was also observed, with an average content of 1.37 % by weight. Other chemical constituents such as Na, Mg, P, S, K, Ca, Cl, Ti, Cr, Mn, Co, Ni, Zn, Pb, Cu, Mo were present in several percent. Rare earth elements such as Pr, Ce, Nd, and Sm were also occasionally found in the particles.
13. As part of Task 3.2, physico-chemical analyses of post-mining waste separation products were carried out on a laboratory scale to determine the possibility of their use in the project and possible directions for their management. The

following analyses were carried out: proximate and ultimate analysis, determination of characteristic ash fusion temperatures, chemical ash composition, microscopic evaluation (using a polarizing microscope) of the mining waste material to determine degree of organic matter degradation, content of trace elements and metals. Based on the physico-chemical analyses carried out, a carbon bearing fraction was selected for testing the gasification process. The material selected was from the Panwenicka heap - HALDEX. It was characterised by the highest calorific value (c.a. 26 MJ/kg), high content of carbon, hydrogen and volatile content. In the case of the mineral fraction, analyses showed that it is also suitable for the geopolymerisation process - it has the correct Na_2O/Al_2O_3 molar ratio. The high levels of silicon and aluminium in all the mineral fraction samples tested indicate the potential for the waste to be used in the production of high value added geopolymeric materials. The characteristic ash fusion temperatures of the samples tested, both for the carbon-bearing product and mineral fractions, exceed 1200°C, which allows us to conclude that agglomeration and slagging problems will not occur when roasting these fractions in the fluidised bed reactor. Microscopic morphological analysis of the enriched mining waste samples did not reveal any visible changes indicating that the organic matter contained in the waste had undergone any thermal or chemical transformations. The laboratory tests carried out also provide the input data for the development of a mine waste beneficiation system (developed by Leader - KOMAG).